SIMPLE INSTRUMENTATION

FOR LARGE FIRES

By

DUANE CLARK MCCOY

Bachelor of Science

University of Tulsa

Tulsa, Oklahoma

1967

Submitted to the faculty of the Graduate College
of the Oklahoma State University
in partial fulfillment of the requirements
for the Degree of
MASTER OF SCIENCE
May, 1969

SIMPLE INSTRUMENTATION

FOR LARGE FIRES

Thesis Approved:

Kenneth P. Bee
Thesis Adviser

Robert H. Johnson, Jr.

D. D. Durham
Dean of the Graduate College

ACKNOWLEDGMENT

I am greatly indebted to Dr. Kenneth J. Bell for his advice and patient guidance throughout my thesis work. I would also like to express my appreciation to Dr. Earl L. Dowty for his help and assistance with the numerical solution to the transient heat conduction problem found in the appendix of this thesis. My gratitude to the members of my graduate committee, to the staff of the School of Chemical Engineering and to my fellow graduate students is also acknowledged.

Financial support for this project has been gratefully received from the United States Air Force.

Finally, I wish to thank my parents for their encouragement, understanding and financial support during my college career.

TABLE OF CONTENTS

LIST OF TABLES

LIST OF FIGURES

NOMENCLATURE

A	area, ft^2
a	constant defined by equation 75, hr^{-1}
b	constant defined by equation 76, hr^{-1}
c	constant defined by equation 77, hr^{-1}
C	specific heat, BTU $lb_m^{-1} ft^{-1}$
C_i	arbitrary constants where i = 1,2,3, ...m
h	external heat-transfer coefficient, BTU $ft^{-2} hr^{-1} F^{-1}$
h'	internal heat-transfer coefficient, BTU $ft^{-2} hr^{-1} F^{-1}$
k	thermal conductivity, BTU $ft^{-1} hr^{-1} F^{-1}$
ℓ	length, ft
M	mass, lb_m
m	constant defined by equation 46, ft^{-1}
n	constant defined by equations 18 and 47, ft^{-1}
Q	heat flow, BTU
Q_1, Q_2	heat flow defined by equations 11 and 12 respectively, BTU
q	heat flow per unit time and area, BTU $ft^{-2} hr^{-1}$
R,r	radius, ft
$\bar{R}$	average of R_i and R_o, ft
t	temperature, ^oF
V	volume, ft^3
v	velocity, ft hr^{-1}
x,y,z	coordinates
x_1	length of fusible rod melted, ft

x_2 initial length of fusible rod, ft

Greek Symbols

α thermal diffusivity, $ft^2 hr^{-1}$

β constant defined by equation 78, hr^{-1}

δ thickness, ft

η_A heat absorption efficiency defined by equations 15 and 41

η_V vaporization efficiency defined by equation 40

θ time, hr

λ_f latent heat of fusion, BTU lb_m^{-1}

λ_v latent heat of vaporization, BTU lb_m^{-1}

ν temperature difference, ^oF

ρ density, $lb_m ft^{-3}$

ω constant defined by equation 79, hr^{-1}

Subscripts

b values at normal boiling point

c conduction

d dowel

f values at normal melting point

g gas

i,o internal and external values respectively

ℓ liquid

m metal

o initial

r rod

s surroundings

t	total values (total heat absorbed, etc.)
1,2,3	denotes temperature domains

Miscellaneous

d	differential operator
Δ	increment, interval spacing
ln	natural or naperian logarithm
∂	partial differentiation operator
∞	infinite
$\approx$	approximately equal sign
$\int$	integral sign
$>$	is greater than
$\leq$	is less than or equal to
$=$	equals
I_p	modified Bessel function of the first kind, of order p
K_p	modified Bessel function of the second kind, of order p

CHAPTER I

INTRODUCTION

In recent years there has been an increasing amount of interest taken in the characterization of large-scale fires. Both governmental and private agencies have undertaken programs to study the phenomena associated with large fires.

Typical instrumentation used for taking data might consist of the following: Thermocouples and thermistors for measuring temperatures inside the fire, radiometers and pyrometers for measuring radiant heat and temperatures, calorimeters for measuring heat fluxes and heat transfer coefficients, and infrared cameras for external mapping of the fire. This sort of instrumentation is bulky, complicated and expensive. To instrument adequately a large test field with only a thermocouple array is an almost insurmountable task. Many thermocouples are required and keeping track of all the wires is a problem. The added expense of a large number of electronic recorders to supplement the thermocouples is usually prohibitive.

The abundance of precise data which can be obtained with the aid of the aforementioned instruments is at the present not necessary due to the lack of extremely accurate correlations between damage and exposure. What is now required, for a better understanding of large-scale fires, is a statistically significant sampling of data from all regions of the fire (i.e. on a fairly dense mesh), even if the data are relatively im-

precise. Such information as maximum and average temperatures, heat fluxes and heat transfer coefficients experienced by a given surface or the total heat absorbed by a given surface would be valuable.

In preparation for this study a literature search was conducted to determine if simple instrumentation had been developed which could be used in place of complicated electronic gear. It was found that an abundance of complicated instruments for measuring thermal activity now exists, but that relatively few simple non-electronic devices have been proposed. The only simple devices located in the literature are described by Thomas and Smith (21) and McCarter and Broido (15). These devices are analyzed in Chapter IV. It is due to the general lack of simple instrumentation that this study was undertaken.

The purpose of this study is to suggest and analyze apparently feasible devices that will provide partial or complete information on the thermal effects in a fire. Since a large number of devices will be required to provide statistically significant results, the devices must be inexpensive. The proposed instrumentation is self-contained and requires no external electrical readout equipment. Most of the devices are non-electronic and all can be constructed from readily available materials. Each device is mathematically modeled and analyzed.

Due to a lack of time, the construction and laboratory or field testing of the proposed devices was not carried out.

CHAPTER II

DESIGN CONSIDERATIONS

In order to obtain information on the spatial distribution of heat releases and temperatures in large fires, one must instrument a test fire adequately. This means that a large number of thermal sensing devices would be required to yield statistically significant sampling of the fire. At present extremely sensitive and accurate electronic gear is not warranted due to the lack of good correlations between exposure and damage.

Since many instruments are required and many may be destroyed in the test, the instruments should be inexpensive. A cost of $1 to $2 per instrument would be desirable, with a maximum cost of $5 to $10 per instrument. The devices must be simple and easy to install, read and interpret. Finally, ruggedness and reliability are also prerequisites. The instrument must be able to withstand moderate mechanical impacts and the thermal environment of the test area. Most of the proposed devices meet these specifications.

CHAPTER III

PHYSICAL CHANGES OF HEATED MATERIALS

In designing an effective heat sensing instrument which is both cheap and self-contained, one may make use of certain permanent or semi-permanent physical changes in heated materials. Reversible changes associated with heating such as expansion of gases or the change in voltage across a thermocouple junction are of less importance because of the need for a recorder. Permanent changes in structure or form of a material such as vaporization or melting can yield information on temperatures and absorbed heat.

The purpose of this chapter is to acquaint the reader with certain physical changes in materials which can be used as a basis for the operation of a heat or temperature sensing device. The following list is not complete but it serves as a starting point for instrument design.

Expansion and Contraction

Most materials expand when heated and contract when cooled. This intrinsic property of matter has been used as the basis for the design of thermometers for centuries. Liquid-filled thermometers were in existence as early as 1654 (20).

Since the expansion-contraction properties of matter are usually reversible, one needs a recorder to obtain a record of a material's temperature history. This added equipment limits the usefulness of the

expansion phenomenon for temperature sensing. Constant volume devices, which allow a portion of the expanded material to leave but do not allow it to return, might be of some use in measuring maximum temperatures.

Melting

Phase changes can often be used to obtain useful information. Many phase changes take place at a specific temperature with substantial heat absorption or release. A familiar example is the melting of ice at 32 F with a heat of fusion of 144 BTU/lb. Since some materials have large heats of fusion, instruments can be designed to yield information on the amount of heat absorbed at a given temperature.

There are commercially available crayons, lacquers and pellets which melt at certain specified temperatures. Once these materials have melted, a permanent record is made of the temperature reached, either by deformation or by changes in surface appearance.

Vaporization

Vaporization of a pure liquid, like the melting of a pure solid, usually takes place at a specific temperature with an accompanying heat effect. The boiling of water at 212 F with a heat of vaporization of 970 BTU/lb is a good example. The vaporization of a liquid lends itself to the design of instruments which record heat absorbed at a given temperature.

Dehydration

Certain materials form hydrates when exposed to water. The following are examples (heats of reaction are at 77 F and 1 atmosphere pressure

(10)):

$$Na_2CO_3\ (c) + 10H_2O\ (\ell) \rightarrow Na_2\ CO_3 \cdot 10H_2O\ (c) + 39{,}800\ BTU$$

$$CaCl_2\ (c) + 6H_2O\ (\ell) \rightarrow CaCl_2 \cdot 6H_2O\ (c) + 41{,}900\ BTU$$

When the hydrated material is heated, the hydration reaction is reversed and the hydrated water is driven off. The rate of dehydration varies with temperature. Unlike the heat of fusion the heat of dehydration does not have to be absorbed at a specific temperature. Thus, it may be possible to postulate a functional form for the heat flux transient and use the weight loss of heated hydrates to evaluate the coefficients.

Reactions

Endothermic reactions or pyrolysis reactions may be used as the basis for heat absorption instrumentation. The following are familiar simple reactions (heats of reaction are at 77 F and 1 atmosphere pressure (10)):

$$2NaHCO_3\ (c) + 55{,}500\ BTU \rightarrow Na_2CO_3\ (c) + CO_2\ (g) + H_2O\ (g)$$

$$2BaO_2\ (c) + 61{,}500\ BTU \rightarrow 2BaO\ (c) + O_2\ (g)$$

These reactions require the addition of heat and will proceed at increasing rates with increasing temperature. The two aforementioned endothermic reactions were chosen because no chemical analysis is required after the reactions have taken place. A simple weighing of the materials before and after heating will enable one to calculate the extent of the reaction and amount of heat absorbed in the reaction.

Color Changes

The color change of certain materials upon heating can be used as an indication of the temperature. There are commercially available temperature sensitive paints. Several of these paints go through as many as five color changes at successively higher temperatures.

These paints are very useful if one wishes to map the temperature contours in a heated material. Parts such as automobile brake drums or engine cooling fins can be coated with one of these paints. After the part has been heated, the isotherms can be clearly seen. These are the regions of uniform color.

The color change of these paints is mainly dependent on the temperature attained. The length of time to which the paint is exposed to that temperature also has an effect. The manufacturers usually standardize the paints for an exposure period of ten minutes. The temperature which produces a given color change within this interval is the listed temperature for a paint. When it is necessary to depart considerably from the standard time exposure, the paints can be restandardized. Some time correction charts may be obtained from the manufacturer.

Hardness Changes

Many materials, especially alloys, undergo permanent hardness changes when they are heated. These changes are due to structural rearrangement and are very reproducible. However, the hardness changes depend both on the maximum temperature to which the alloys were heated and on the duration of exposure (1).

Magnetic Changes

Magnetic materials usually lose their magnetic properties when they are heated. If no phase change has occurred during the heating, the magnetic properties will be restored as the material is cooled. A magnetic material may be partially or totally demagnitized if it undergoes a phase change upon heating.

If a steel has a martensitic structure, its susceptibility is permanently decreased as the steel ages. This aging proceeds very slowly at room temperature but is accelerated by heating (9). This loss of magnetic properties is due to a change in the martensitic structure of the metal, the tetragonal martensite becoming cubic. The total induction of quenched steel magnets can be reduced by as much as 20 per cent by metallurgical aging (9).

Summary of Physical Changes

In general any permanent or semi-permanent phase change in a material due to heating can usually be used as a basis for a temperature or heat sensing device. Phase changes which take place at specific temperatures, such as melting or boiling, lend themselves to instruments which measure maximum temperature and total heat absorbed at a given temperature.

If one postulates a functional form for the heat flux or temperature transients, then phase changes which take place over various temperature ranges and at various rates might be used to evaluate the coefficients.

Transient reversible changes in heated materials such as expansion may be used in devices which are equipped with recorders, either mechanical or electronic.

CHAPTER IV

EXISTING SIMPLE INSTRUMENTATION

A literature search was conducted in order to determine if simple instrumentation had been developed for measuring thermal effects of fires. Only two promising devices were found. These devices are described in the following discussion.

High-Intensity Thermal Radiometer

Thomas and Smith have proposed a very simple instrument for measuring high-intensity thermal radiation (21). This instrument consists of a sandwich of three metal plates. The first plate has a hole in its center. The second plate is painted with a heat sensitive paint or lacquer and the third plate is used as a heat shield. The meter is illustrated in Figure 1 and nominal dimensions are shown. The appearance of the second plate after heating is also shown.

When thermal radiation is allowed to fall on the restricted area of the second plate, it is conducted outward. The area of paint which has changed color or been melted is taken as a measure of the radiation dosage. This instrument works best for exposures of short duration (a few seconds) and high intensity (10^{1}-10^{2} BTU/ft^{2}-sec). It will probably be of little use in large test fires where exposure times are in minutes or hours and the radiant energy is relatively low (10^{-2}-10^{-1} BTU/ft^{2}-sec) (3).

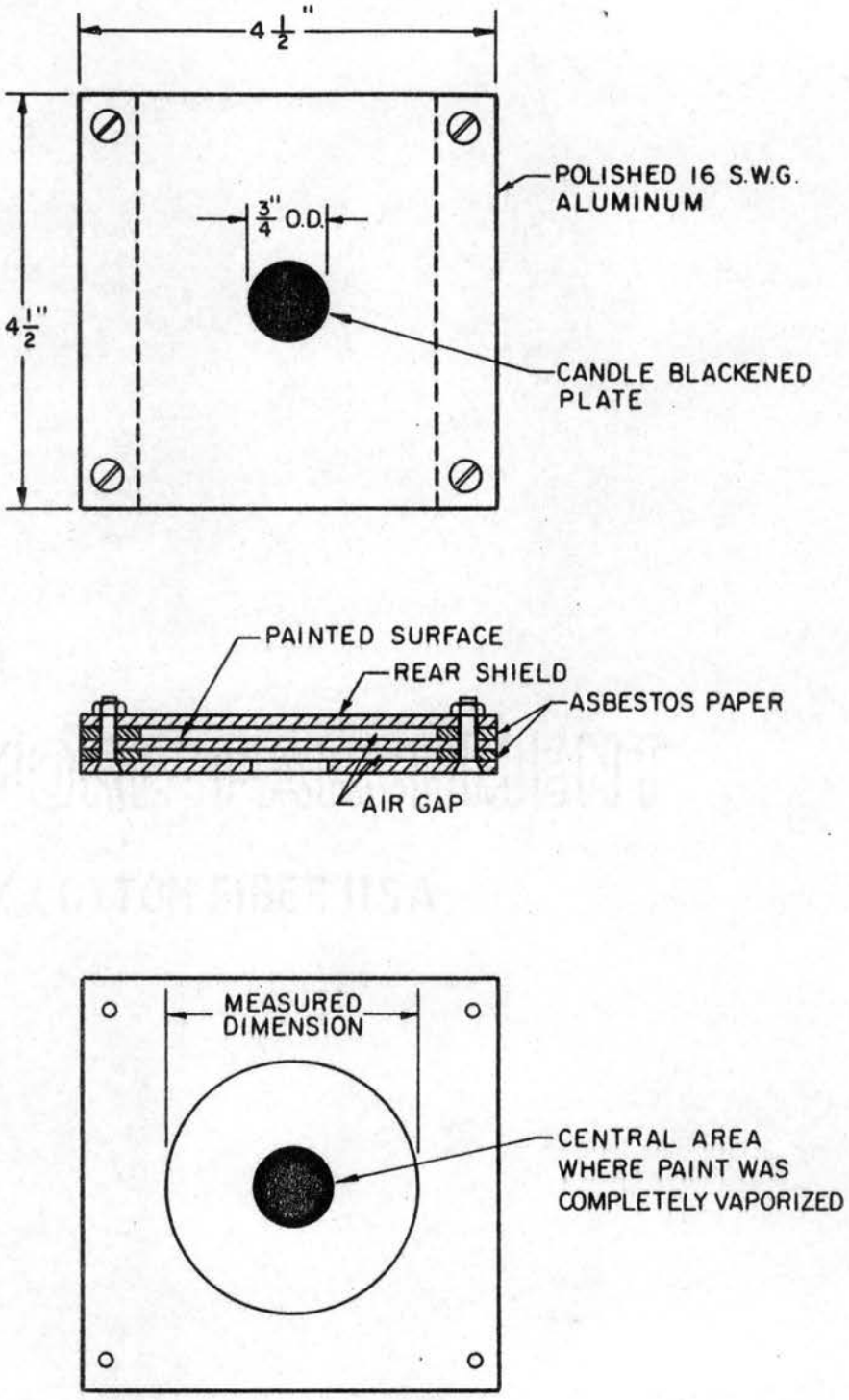

Figure 1. High-Intensity Thermal Radiometer

Radiant Energy Dosimeter

McCarter and Broido have suggested a dosimeter for measuring radiant energy (15). It consists of two identical thin-walled metal containers as shown in Figure 2. Each container is insulated except for one surface. One of the exposed surfaces is painted black and will absorb radiated and convected heat while the other is polished and will reflect radiated heat. The containers are filled with equal volumes of liquid and placed in a hot-fire environment. As long as some liquid remains in the containers, the temperature of the containers is approximately the bubble point of the liquid. Thus, the convective heat transfer remains the same for both containers. By measuring the weight of liquid lost due to evaporation for each container and taking the difference, the total radiated heat seen by the exposed surfaces can be calculated.

There are several inherent limitations in the design of the instrument. A simple mathematical modeling of the instrument requires that the absorptances of the respective surfaces remain constant. This condition may not exist if contaminants are deposited on the exposed surfaces when the device is subjected to a fire environment.

If the liquid in the two containers must be heated from ambient temperature to its boiling temperature, then the time involved in reaching the boiling temperature will be different for the two containers. As long as the cooler reflecting container is below the boiling temperature, the convected heat transferred to it will be greater than that to the black. Finally if the ambient gas temperature drops below the meter temperature, the convective energy transfer will be from the heated meter to the surroundings. This can seriously affect the radiant energy detection. An instrument in the periphery of the fire will be

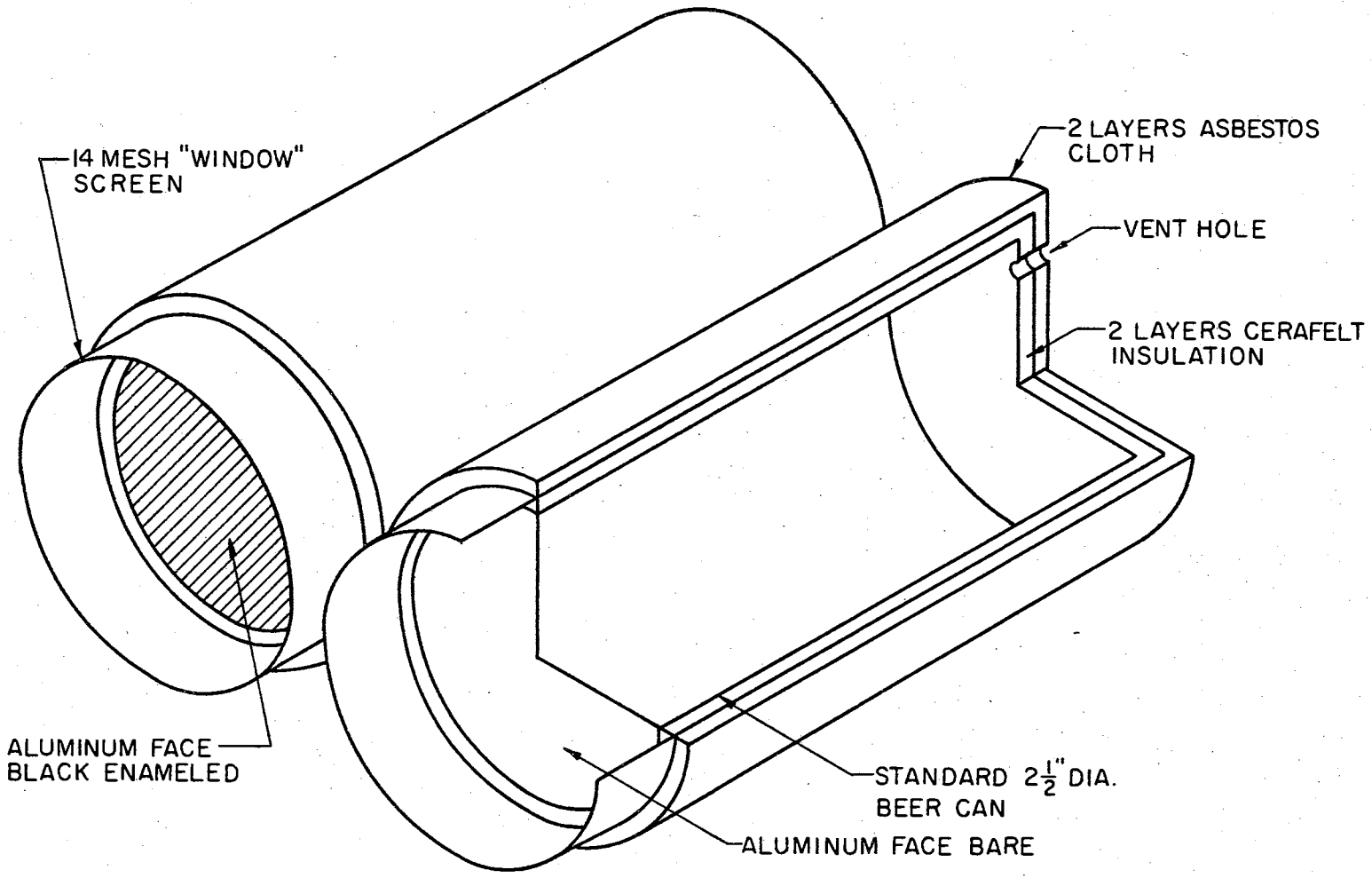

Figure 2. Radiant Energy Dosimeter

more susceptible to this error than an instrument in the interior of the fire.

Despite this instrument's limitations useful information can probably be obtained from it. An adaptation of this instrument is described in the following chapter on proposed instrumentation.

CHAPTER V

PROPOSED INSTRUMENTATION

The purpose of this chapter is to suggest and analyze apparently feasible instrumentation for the measurement of the thermal properties of large fires. The suggested instruments all theoretically fulfill, to a greater or lesser degree, the design specifications given in Chapter II. They are inexpensive, simple in design and operation and relatively rugged.

Designs which were initially suggested as being feasible but which upon further examination proved to be unsatisfactory, are also included.

Maximum Temperature Indicator

Perhaps the simplest measuring instrument is a maximum temperature indicator. Such a device is illustrated in Figure 3. It consists of a foamed silica dowel or tube wrapped with aluminum foil. Rings of different heat sensitive lacquers are painted on the aluminum foil. Each lacquer ring will melt at a specific temperature. Once a lacquer has melted it may be easily recognized from non-melted lacquer even after it has resolidified.

These devices can be scattered throughout a test range and retrieved for examination after the fire has burned out. The maximum temperature reached by the device is taken to be the melting temperature of the highest rated, melted lacquer. In other words, if the aluminum foil was

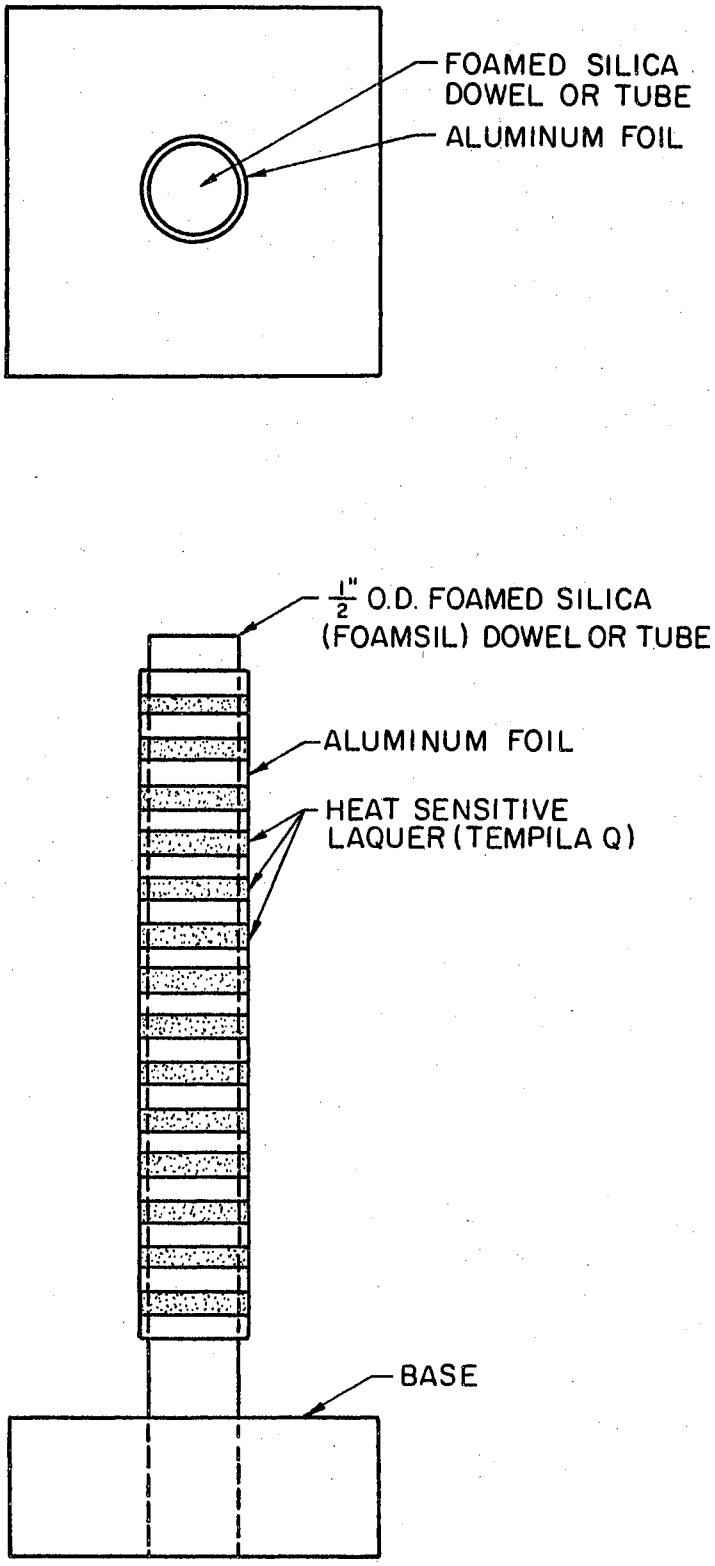

Figure 3. Maximum Temperature Indicator

painted with nine different lacquers, whose melting points were at 100 F increments from 200 F to 1000 F, and was then exposed to a temperature of 825 F, all the lacquers with melting points of 800 F or below would be melted. All of the lacquers whose melting points were above 825 F would not be melted. Therefore, the temperature reached by the device is known to have been at least 800 F and can be assumed to be 850±50 F. The accuracy of the instrument may be easily adjusted by selecting different temperature increments between the melting points of the lacquers.

If maximum temperatures in excess of 1200 F are to be measured, then steel or stainless steel should be used in place of the aluminum foil.

By neglecting the heats of fusion of the melting lacquers and assuming that no temperature gradients exist in the foil, the foil may be analyzed as a solid of infinite thermal conductivity. Eckert and Drake give the following equation for Newtonian heating and cooling of a solid in a constant temperature environment (4):

$$\frac{t-t_s}{t_o-t_s} = e^{-hA_m\theta/(\rho_m C_m V_m)} \qquad (1)$$

where

A_m = exposed surface area of the metal foil

C_m = specific heat of metal foil

h = heat-transfer coefficient to the foil

t = temperature

t_o = initial temperature

t_s = temperature of the surroundings

V_m = volume of metal foil

θ = time of heating

ρ_m = density of metal

Equation 1 may be used to predict the time-temperature response of the instrument. Since $\rho_m V_m$ is actually a mass term, the ρ_m should be evaluated at the temperature at which V_m and A_m were measured. This is usually at initial conditions. The specific heat of most metals may be represented as a linear function of temperature. Therefore, C_m should be evaluated at the average metal temperature during the heating.

Example 1. An instrument similar to the one shown in Figure 3 is exposed in a fire. A 1/2 inch diameter by 6 inch foamed silica dowel is wrapped with a thin (.001 inch thick) aluminum foil. (a) calculate time required to heat the aluminum foil to within ten per cent of the surrounding hot gas temperature. Neglect the heat conduction into the foamed silica dowel. (b) estimate the time required to heat the aluminum foil if the heat conduction into the foamed silica dowel is not neglected.

Given:

A_m	0.0654 ft^2
C_d	0.2480 BTU/lb-F
C_m	0.2470 BTU/lb-F
h	25 BTU/ft^2-hr-F
k_d	0.107 BTU/ft-hr-F
t	1080 F
t_o	80 F
t_s	1200 F
V_m	5.45×10^{-6} ft^3
ρ_d	11 lb/ft^3

ρ_m 169 lb/ft^3

The subscripts m and d refer to the metal foil and to the foamed silica dowel, respectively. The physical properties of the aluminum and the foamed silica were taken from references (5) and (16).

(a) After solving equation 1 for time and then substituting the given data, a response time of 3.1×10^{-4} hours or 1.1 seconds is calculated. Thus, it is noted that the theoretical response time is short.

(b) Heat conduction into the foamed silica dowel will now be considered. Since the aluminum foil is thin and has a high thermal conductivity (120 BTU/ft-hr-F), it may be considered to be at a uniform temperature throughout. It will be assumed that the aluminum foil offers no resistance to heat conduction and that the temperature of the foil and the surface of the dowel are the same. The problem is to calculate the time required to heat the outside surface of the dowel to 1080 F. The heating time may be calculated with the aid of the Boelter charts for one-directional transient heat conduction in solid cylinders (2). These charts show $(t-t_s)/(t_o-t_s)$ as a function of $(\alpha_d \theta/r_d^2)$ with $k_d/(hr_d)$ as a parameter. Here α_d is the thermal diffusivity $k_d/(\rho_d C_d)$ of the dowel and r_d is the radius. An example of the application of these charts is given in the text by Eckert and Drake (4).

From the statement of the problem and the given information, the following expressions were calculated:

$$\frac{t-t_s}{t_o-t_s} = 0.1072$$

and

$$\frac{k_d}{hr_d} = 0.2055$$

The Boelter charts yield

$$\frac{\alpha_d \theta}{r_d^2} = 0.21$$

Then

$$\theta = 8.4 \text{ seconds}$$

Example 1 shows that a thin metal foil may be rapidly heated from some initial temperature to within a few per cent of the surrounding temperature. The actual response time for an instrument exposed to similar conditions will probably be between the values given in parts (a) and (b) of the example. Heat losses from fusion of the heat-sensitive lacquers will tend to increase the response time while the thin layer of air between the foil and the dowel will tend to insulate the dowel from the foil and decrease the response time.

The materials for constructing the device are readily available. The foamed silica (Foamsil) may be obtained from Pittsburgh Corning. Heat-sensitive lacquers known as Tempilaqs may be purchased from the Tempil Corporation. These lacquers melt rapidly when they are heated to their rated temperatures. Heat-sensitive paints which change color upon heating are also available. The use of these paints is not recommended because they exhibit a time as well as a temperature dependence for their color changes.

The painting of the metal foil with the heat-sensitive lacquers offers some minor difficulties. Painting of long sheets of metal foil with parallel stripes of the lacquers is suggested. Many small metal foils large enough to wrap around the silica dowels may be cut from the

large painted sheet. A template made from cardboard or plastic might also be used to aid in the painting. Care must be taken in keeping the heat-sensitive lacquers from mixing with each other. If they are allowed to mix with one another, their melting points will be changed.

Finally, this device seems to be a practical solution to the problem of measuring the maximum temperature reached by any point in a fire. The device is simple, inexpensive and rugged. The foam silica core may be used many times by simply replacing the old lacquered foil with a new one.

Fusible-Rod Integrated-Heat Flux Meter

The simple device shown in Figure 4 may be used to measure the total amount of heat absorbed by a surface at a given temperature. Basically the instrument is a metal disk, on which heat is absorbed, and a fusible rod which removes the heat absorbed by the metal plate. The fusible rod is made from a material which has a specific melting point. Once the rod begins to melt, it acts as a coolant and keeps the heat-absorbing surface at or near the melting temperature of the fusible rod. Shortly after the metal plate has reached the melting point temperature of the fusible rod, melting of the rod will occur on the common surface between the rod and the metal disk. As melted material falls away, the metal plunger and compression spring push new material to the heated surface.

If the fusible rod and its container are properly covered with a good insulating material, such as laminated asbestos felt, then most of the heat conducted to the rod will be through the metal disk.

During a test the device may be completely submerged in a flame.

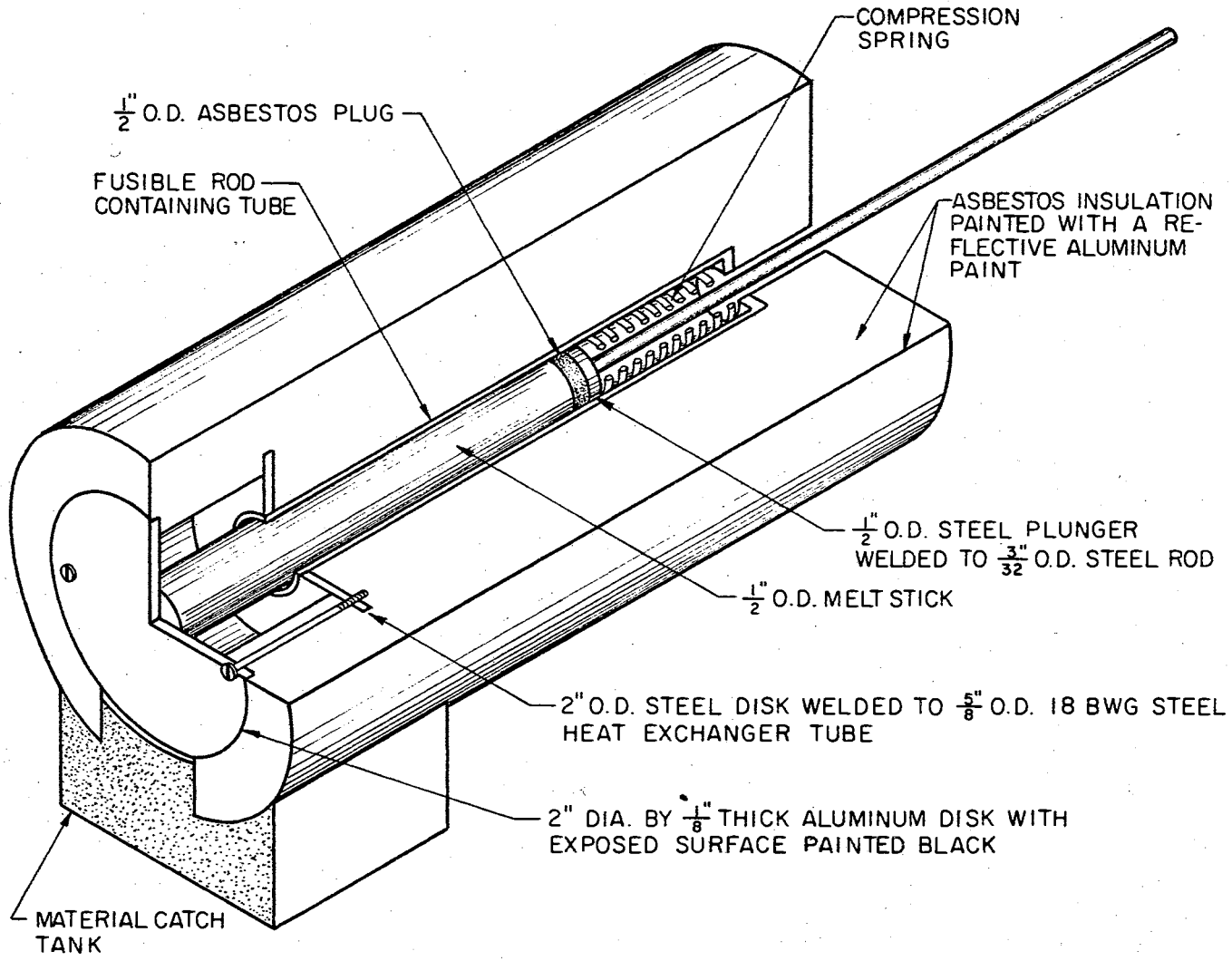

Figure 4. Fusible-Rod Integrated-Heat Flux Meter

A metal "catch" tank is attached below the exhaust opening for the melted material. This material reservoir serves as a heat shield and keeps the fusible rod from being exposed to a direct flame.

The length of steel rod which extends out of the surrounding insulation is used to measure the amount of fusible rod consumed during a test. This can facilitate the data gathering process. Before a test the protruding rod is marked at the point where it enters the insulating covering. After the test has been conducted the rod is again marked where it enters the insulation. The distance between the two markings is the length of the fusible rod which has been melted.

The metal disk is made from a metal which has a high thermal conductivity, such as aluminum or copper. This is done so that the temperature gradients in the metal are minimized.

In the following derivations the subscripts (m) and (r) shall refer to the exposed metal and to the fusible rod respectively. The heat absorbed through the exposed metal surface is

$$Q_t = hA_m \int_o^{\theta} (t_s - t_m) d\theta \qquad (2)$$

This energy must be absorbed by the metal plate and the fusible rod. Temperature gradients are assumed not to exist in the exposed metal disk. Once the metal disk has reached the melting temperature of the fusible rod, the disk is assumed to remain at that temperature as long as melting of the rod continues. Therefore, if x_1 denotes the length of fusible rod which has been melted, then the total heat absorbed through the exposed metal surface is

$$Q_t = \pi R_m^2 \delta_m \rho_m \int_{t_o}^{t_f} C_m dt + \pi R_r^2 x_1 \rho_r \left[\int_{t_o}^{t_f} C_r dt + \lambda_f \right] + Q_c \qquad (3)$$

where λ_f, Q_c, t_f and δ_m are the latent heat of fusion of the rod, the heat conducted along the rod, the melting temperature of the rod and the thickness of the exposed metal plate respectively. If the specific heats are constant, equation 3 reduces to

$$Q_t = \pi\left[(R_m^2\delta_m\rho_m C_m + R_r^2 x_1 \rho_r C_r)(t_f - t_o) + R_r^2 x_1 \rho_r \lambda_f\right] + Q_c \qquad (4)$$

The $\pi R_m^2 \rho_m \delta_m$ and $\pi R_r^2 x_1 \rho_r$ terms are masses; therefore, ρ_m and ρ_r should be evaluated at the temperature at which the dimensions R_m, R_r and δ_m are measured. This is usually the initial temperature (room temperature). All other physical properties such as specific heat C and thermal conductivity k should be evaluated at the average temperature between t_o and t_f.

The variable t_m in equation 2 may be assumed to be constant and equal to t_f if the energy absorbed by heating the metal disk to t_f is relatively small when compared with the energy absorbed by melting the rod. The variables h and t_s may not generally be known. Therefore, integration of equation 2 may not be possible. Equation 4 offers an indirect method for evaluating the integral of equation 2.

The conduction term of equation 4 represents the amount of heat which has been conducted into the remaining non-melted portion of the fusible rod. In order to calculate this term one must evaluate the temperature profile along the length of the remaining rod.

As the rod melts the remaining portion of the rod is moved toward the heated metal surface. This procedure may be visualized as a heat source moving along a stationary rod. The following assumptions will be made:

(1) The physical properties of the fusible rod are independent

of temperature.

(2) The velocity of melting v and the rate of heat input q are constant.

(3) Heat flow is linear along the axis of the rod with no radial temperature gradients.

(4) The rod is infinitely long.

With these assumptions the exact analytical theory was worked out by Rosenthal (17). The temperature at any point along the length of the rod is

$$t = t_o + (t_f - t_o)e^{-\frac{v}{\alpha_r}(x-v\theta)} \tag{5}$$

where α_r is the thermal diffusivity of the rod and x is some rod length greater than $(v\theta)$. If x is substituted for $v\theta$, equation 5 reduces to

$$t = t_o + (t_f - t_o)e^{-\frac{v}{\alpha_r}(x-x_1)} \tag{6}$$

The assumption that the rod is infinitely long does not literally have to be met. As long as the fusible rod's unheated surface remains essentially at t_o, the rod can be considered to be infinitely long.

The amount of heat conducted down the rod can now be calculated.

$$Q_c = \pi R_r^2 \rho_r C_r \int_{x_1}^{x_2} (t-t_o)dx \tag{7}$$

Here x_1 and x_2 are the melted and initial lengths of the fusible rod respectively. Equation 5 is substituted for the value of t in equation 7 yielding

$$Q_c = \pi R_r^2 \rho_r C_r (t_f - t_o) \int_{x_1}^{x_2} e^{-\frac{v}{\alpha_r}(x-x_1)} dx \tag{8}$$

Equation 8 is integrated and reduced to

$$Q_c = \pi R_r^2 k_r \frac{(t_f - t_o)}{v} \left[1 - e^{-\frac{v}{\alpha_r}(x_2 - x_1)}\right] \quad (9)$$

Finally, equation 9 is substituted into equation 4. Thus

$$Q_t = \pi\left[R_m^2 \delta_m \rho_m C_m + R_r^2 \rho_r C_r x_1 + \frac{R_r^2 k_r}{v}\left(1 - e^{-\frac{v}{\alpha_r}(x_2 - x_1)}\right)\right](t_f - t_o) + \pi R_r^2 \rho_r x_1 \lambda_f \quad (10)$$

If the fusible rod is made from a material with a low thermal conductivity, then Q_c may usually be neglected. This simplifies equation 10 considerably and eliminates difficulties which would be encountered in measuring the rate at which the rod melts. In actual operation, the heat input will generally not be constant. Therefore, the rate at which the rod melts will not be constant. If the velocity is considered to be a function of the time then the equations used to derive equation 6 become non-linear. A numerical solution for the conduction term would probably be required. Thus, it is advantageous to be able to neglect the conduction term.

An example will now be given to illustrate the minuteness of the conduction term in equation 10 and to justify neglecting this term.

Example 2. A fusible-rod integrated-heat flux apparatus which is initially at 80 F is placed in an oven for one minute and then removed. The temperature inside the oven is 1000 F and the heat-transfer coefficient is 25 BTU/ft^2-hr-F. The heat absorbing surface of the fusible-rod apparatus is a 2 inch diameter by 1/8 inch thick aluminum disk. The 1/2 inch diameter by 8 inch fusible rod is made from β-naphthol. The temperature is assumed to be uniform throughout the exposed metal surface and heat conduction through the insulation is neglected. Calculate (a) the time required to heat the exposed metal plate to the melting

temperature of the fusible rod, (b) the total heat absorbed through the exposed metal surface, (c) the amount of fusible rod consumed during the heating, (d) the amount of heat conducted down the remaining portion of the fusible rod and (e) the temperature profile in the remaining non-melted rod.

Given:

C_m	0.228 BTU/lb-F
C_r	0.345 BTU/lb-F
k_m	120 BTU/ft-hr-F
k_r	0.139 BTU/ht-hr-F
t_f	249 F
λ_f	56.4 BTU/lb
ρ_m	169 lb/ft^3
ρ_r	76 lb/ft^3

The physical properties of aluminum and β-naphthol were taken from references (5, 11, 14).

(a) The time required to heat the aluminum disk to 249°F is calculated by solving for time in equation 1. Thus,

$$\theta_1 = 11.7 \text{ sec}$$

(b) The energy required to heat the aluminum disk to 249°F is

$$Q_1 = \pi R_m^2 \delta_m \rho_m C_m (t_f - t_o) \tag{11}$$

$$Q_1 = 1.48 \text{ BTU}$$

The fusible rod is assumed to begin melting with a velocity v and the temperature of the metal surface is assumed to remain at 249°F for the next 48.3 seconds, θ_2. The heat added during this time is

$$Q_2 = \pi h R_m^2 (t_s - t_f)\theta_2 \tag{12}$$

$$Q_2 = 5.51 \text{ BTU} \tag{11}$$

The total heat abosrbed by the metal surface during the minute exposure is

$$Q_t = Q_1 + Q_2 \tag{13}$$

$$Q_t = 6.99 \text{ BTU} \tag{10}$$

(c) The length of fusible rod melted can now be calculated from equation 10. Since equation 10 is transcendental with respect to x_1, the calculation involves a trial and error procedure. First, x_1 is assumed and the velocity v is calculated.

$$v = x_1/\theta_2 \tag{14}$$

These values for x_1 and v are substituted into equation 10 and Q is calculated. This Q is then compared with the Q_t calculated from equation 13. If Q equals Q_t then the correct x_1 was chosen. If Q does not equal Q_t then another x_1 is chosen. This procedure is continued until the correct x_1 is chosen. The final value for x_1 is 5.58 inches.

(d) From equation 9 the amount of heat conducted down the remaining portion of the fusible rod is calculated to be approximately 1×10^{-3} BTU.

(e) Finally, the temperature profile down the remaining length of rod is calculated from equation 5. Figure 5 shows the results of this calculation. This temperature profile indicates that heat penetrates only a short distance from the heated surface into the fusible rod.

The heat conduction down the fusible rod has been shown to be small when compared with the other heat absorption terms. Therefore, it should usually be permissible to neglect the conduction term of

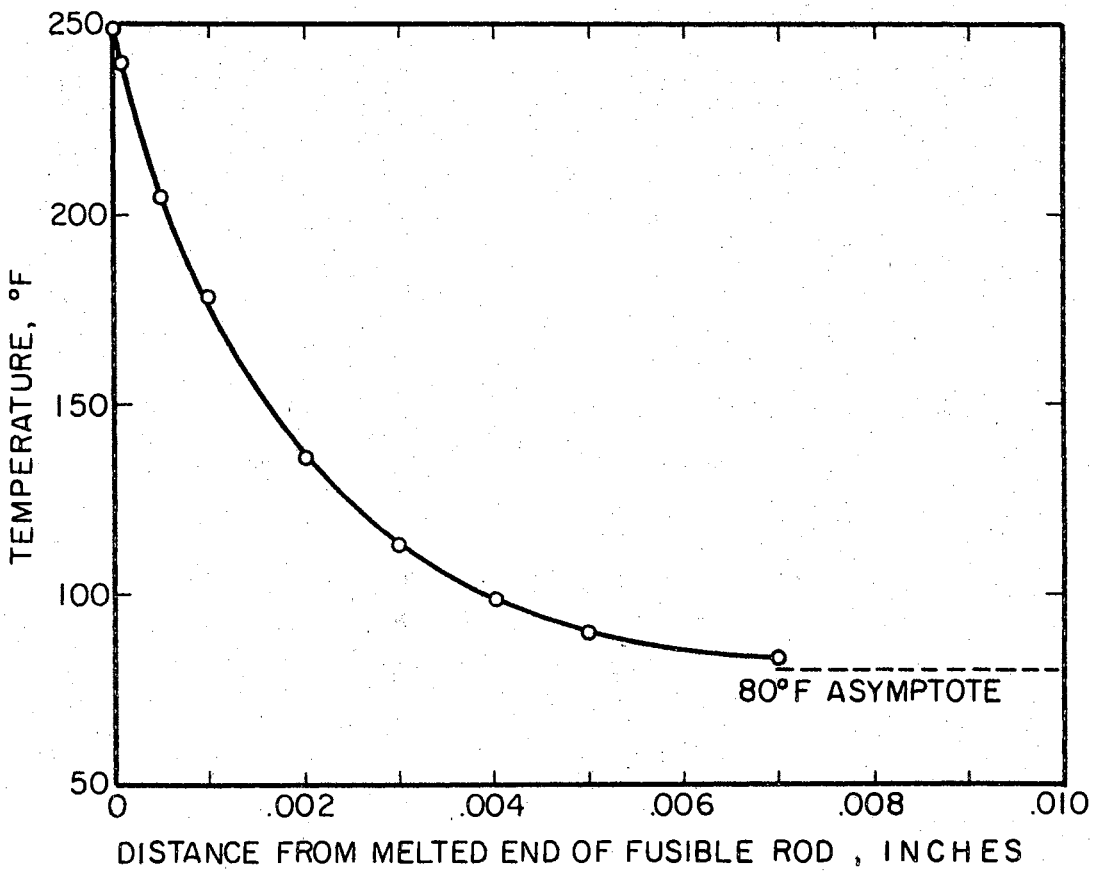

Figure 5. The Temperature Profile in the Non-Melted Portion of the Fusible Rod

equation 10.

The calculation of example 2 was for an instrument which had no temperature gradients in the exposed metal surface. Actual instruments will have some radial temperature gradients in this surface and will not be as efficient as the example instrument. The following derivation is an attempt to predict the efficiency of the exposed metal surface.

The efficiency of the metal surface will be defined as the ratio of the total heat absorbed by the metal disk to that which would be absorbed if the entire exposed surface were at t_f. If radiation is neglected, then the heat absorption efficiency is defined as

$$\eta_A = \frac{2}{(t_\delta - t_f)R_m^2} \int_o^{R_m} (t_s - t_m) r \, dr \qquad (15)$$

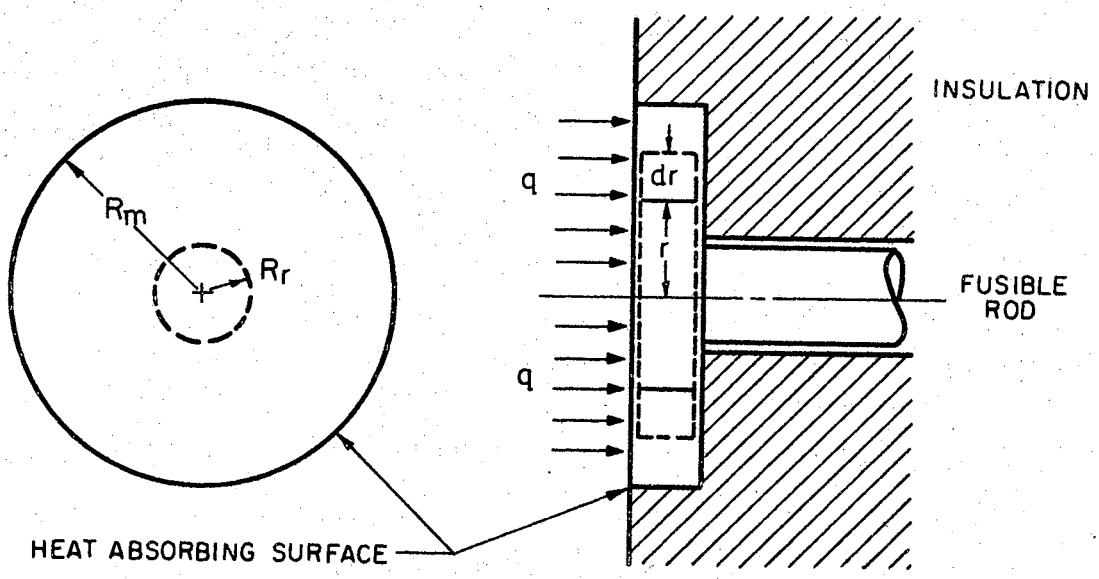

Figure 6. Fusible-Rod Integrated-Heat Flux Meter Schematic

In order to evaluate equation 15 the radial temperature profile in the metal disk must be calculated. This may be done by setting up and evaluating the conduction equation for the exposed metal disk. Figure 6 is a schematic of the fusible-rod apparatus and may be referred to in order to visualize the conduction process.

As heat is absorbed by the metal surface it is conducted to and absorbed by the fusible rod. Only radial temperature gradients are considered to exist in the metal disk. The heat-transfer coefficient h is assumed to be a constant. If ν is defined as $t_s - t_m$, then the time independent (steady state) heat conduction equation for the disk may be written as

$$\frac{d^2\nu}{\partial r^2} + \frac{1}{r}\frac{d\nu}{dr} - \frac{h\nu}{k_m \delta_m} = 0 \qquad (16)$$

Equation 16 is recognized as a form of Bessel's equation. The solution to equation 16 is

$$\nu = C_1 I_o(nr) + C_2 K_o(nr) \tag{17}$$

where

$$n = \sqrt{h/(k_m \delta m)} \tag{18}$$

The heat conduction problem is now broken into two parts. The projected area of the fusible rod on the exposed surface is assumed to be at a uniform temperature t_f. Thus only radial temperature gradients exist in the portion of the exposed surface between R_r and R_m. The arbitrary constants C_1 and C_2 in equation 17 are now evaluated by applying the following boundary conditions:

$$(1)\ \nu_f = t_s - t_f \text{ at } r = R_r$$

$$(2)\ \frac{d\nu}{dr} = 0 \text{ at } r = R_m$$

Therefore,

$$C_1 = \frac{\nu_f K_1(nR_m)}{K_1(nR_m) I_o(nR_r) + I_1(nR_m) K_o(nR_r)} \tag{19}$$

$$C_2 = \frac{\nu_f I_1(nR_m)}{K_1(nR_m) I_o(nR_r) + I_1(nR_m) K_o(nR_r)} \tag{20}$$

The efficiency of the exposed surface is calculated by breaking the integral of equation 15 into two parts. Hence

$$\eta_A = \frac{2}{\nu_f R_m^2} \left[\nu_f \int_o^{R_r} r\, dr + \int_{R_r}^{R_m} (C_1 I_o(nr) + C_2 K_o(nr)) r\, dr \right] \tag{21}$$

$$\eta_A = \frac{nR_r^2 + 2\left[\frac{C_1}{\nu_f}(R_m I_1(nR_m) - R_r I_1(nR_r)) - \frac{C_2}{\nu_f}(R_m K_1(nR_m) - R_r K_1(nR_r))\right]}{nR_m^2} \tag{22}$$

Equation 22 is further reduced by defining two new constants, C_3 and C_4.

$$C_3 = \frac{C_1}{\nu_f} \tag{23}$$

$$C_4 = \frac{C_2}{\nu_f} \tag{24}$$

Hence, equation 22 reduces to

$$\eta_A = \frac{nR_r^2 + 2\left[C_3(R_m I_1(nR_m) - R_r I_1(nR_r)) - C_4(R_m K_1(nR_m) - R_r K_1(nR_r))\right]}{nR_m^2} \tag{25}$$

It should be noted that there are no temperature terms in equation 25. Thus for any specifically dimensioned disk of a given material, the efficiency is only a function of the heat-transfer coefficient.

Equation 25 may be used to evaluate the relative effectiveness of various surfaces. As an illustration, consider Figure 7. The efficiency curves were generated by equation 25. Figure 7 shows the efficiencies of various 1/8 inch thick aluminum disks as functions of the external heat-transfer coefficient, from equation 25. The efficiency of the exposed metal surface is clearly seen to decrease with any increase in the heat transfer to that surface and with any increase in the radius of that surface.

Example 3. Calculate (a) the heat absorption efficiency of the instrument which is described in Example 2. Estimate (b) the total heat absorbed by the exposed metal surface and (c) the actual amount of the fusible rod consumed in the instrument.

(a) Once melting has started the heat absorption efficiency of the exposed metal surface may be calculated directly from equation 25 yielding

$$\eta_a = .954$$

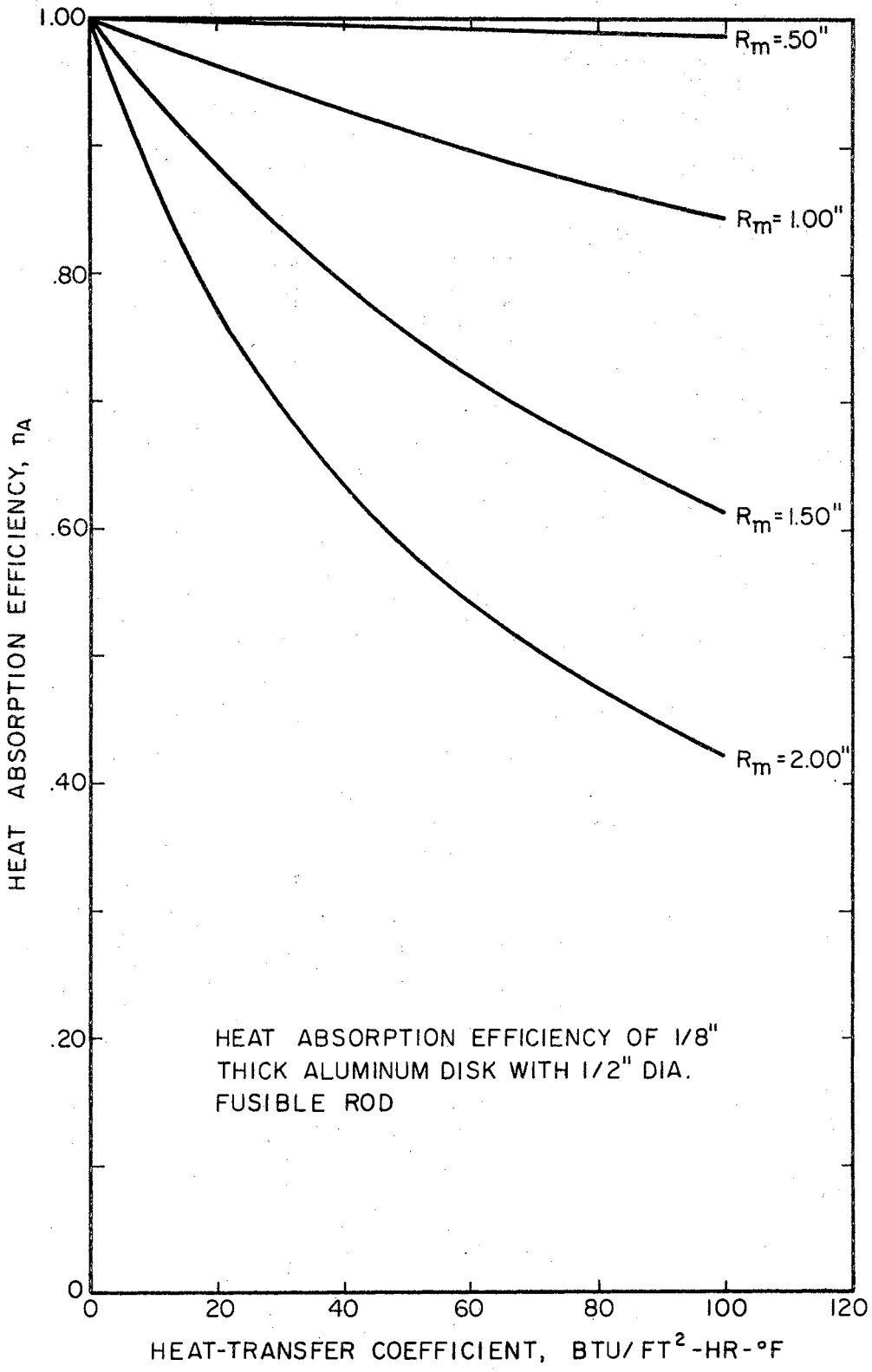

Figure 7. Heat Absorption Efficiency of Exposed Metal Surface

(b) The instrument described in Example 2 is an "ideal" device with an infinite k_m. When melting has started, the heat absorption efficiency of this device is 1.0. To estimate the total heat absorbed by the "real" device, the real device will be assumed to be 95.4 per cent as efficient as the ideal device over the total heating period. The total heat absorbed by the instrument is estimated to be

$$Q_t = \eta_A(Q_1 + Q_2)$$

$$Q_t = 6.66 \text{ BTU} \tag{26}$$

(c) After the instrument has been removed from the oven, radial temperature gradients will still exist in the exposed metal disk. Because of these temperature gradients excess heat is stored in the metal disk. This excess heat is assumed to be rapidly conducted to the fusible rod. When the excess heat has been absorbed by the fusible rod melting ceases. At the instant the melting ceases the average temperature of the exposed metal disk is very near the melting temperature of the fusible rod. Therefore, if the conduction along the fusible rod can be nelgected, then the length of fusible rod consumed during a test can be calculated by solving for x_1 in equation 10.

$$x_1 = \frac{Q_t - \pi R_m^2 \delta_m \rho_m C_m (t_f - t_o)}{\pi R_r^2 \rho_r (C_r (t_f - t_o) + \lambda_f)}$$

$$x_1 = 5.24 \text{ in.} \tag{27}$$

After an actual field test, the amount of fusible rod consumed in an instrument would be known and the heat absorbed by an "ideal" instrument would be unknown. If the average heat absorption efficiency can be estimated, then the heat which would have been absorbed by an "ideal"

instrument can be estimated from equation 28.

$$Q = \frac{\pi\left[\left(R_m^2 \delta_m \rho_m C_m + R_r^2 \rho_r C_r x_1\right)(t_f - t_o) + R_r^2 x_1 \rho_r \lambda_f\right]}{\eta_A} \tag{28}$$

The conduction of heat along the fusible rod is again assumed to be negligible.

For the instrument described in Example 2, the heat conduction through the surrounding insulation to the fusible rod was assumed to be negligible. The validity of this assumption depends on the type and thickness of the insulation. To insure that the instrument is properly protected one should design the insulation for the most severe conditions which the instrument will be subjected to. One possible set of conditions might be:

(1) The instrument and the surrounding insulation are initially at 80 F.

(2) The temperature of the inside surface of the insulation is not to exceed 200 F at any time.

(3) The surrounding temperature is 1000 F.

These conditions were used as a basis for Figures 8 and 9. The figures were constructed with the aid of the Boelter charts for one-directional transient heat conduction in solid cylinders and slabs (2). Figures 8 and 9 enable one to determine the amount of insulation which may be required to keep an instrument cool for various time increments. The figures also show that the heat conducted through the insulation is relatively independent of the surrounding heat-transfer coefficient. This indicates that the heat conducted through the insulation is pri-

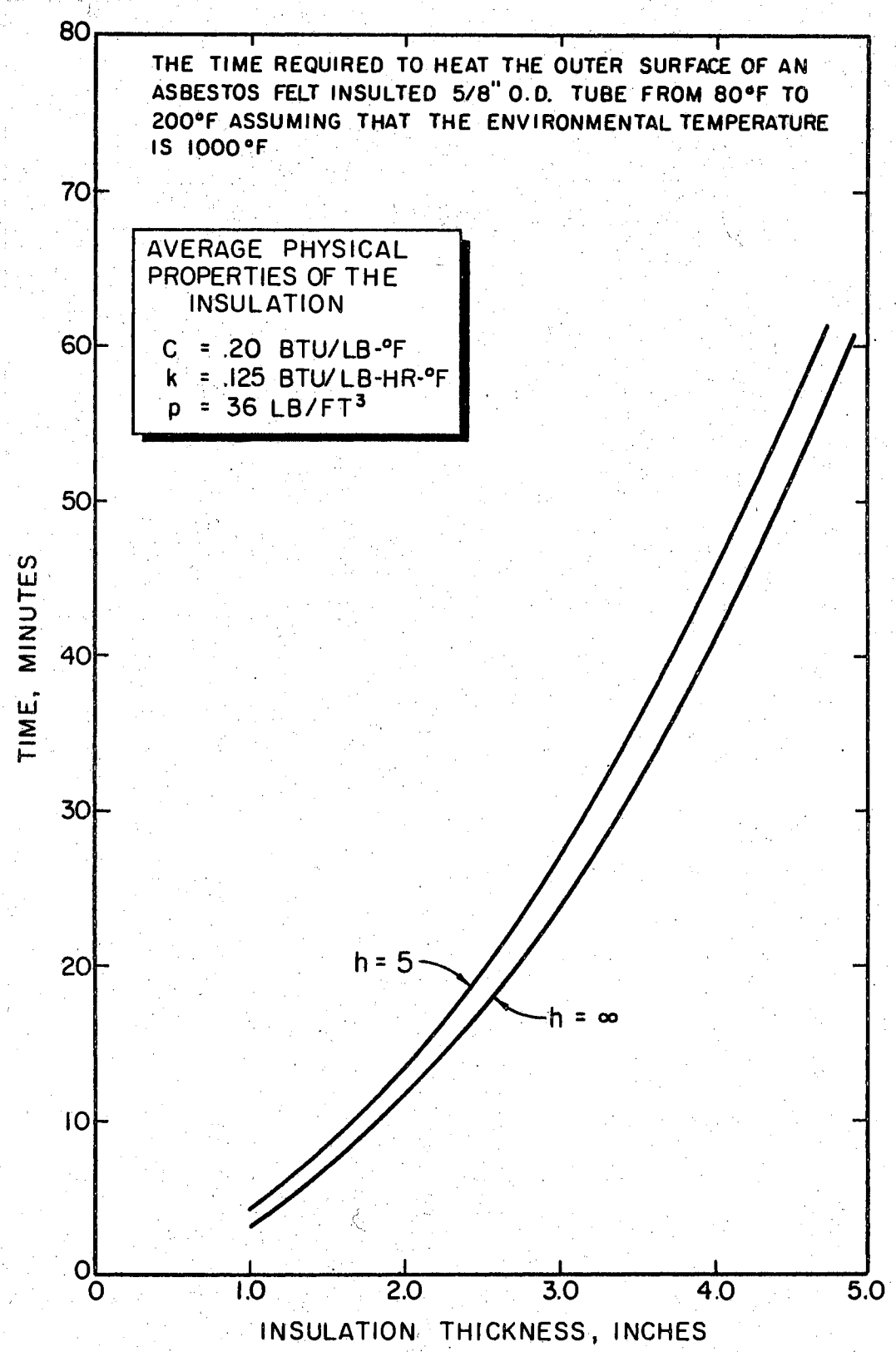

Figure 8. Cylindrical Shell Insulation Thickness

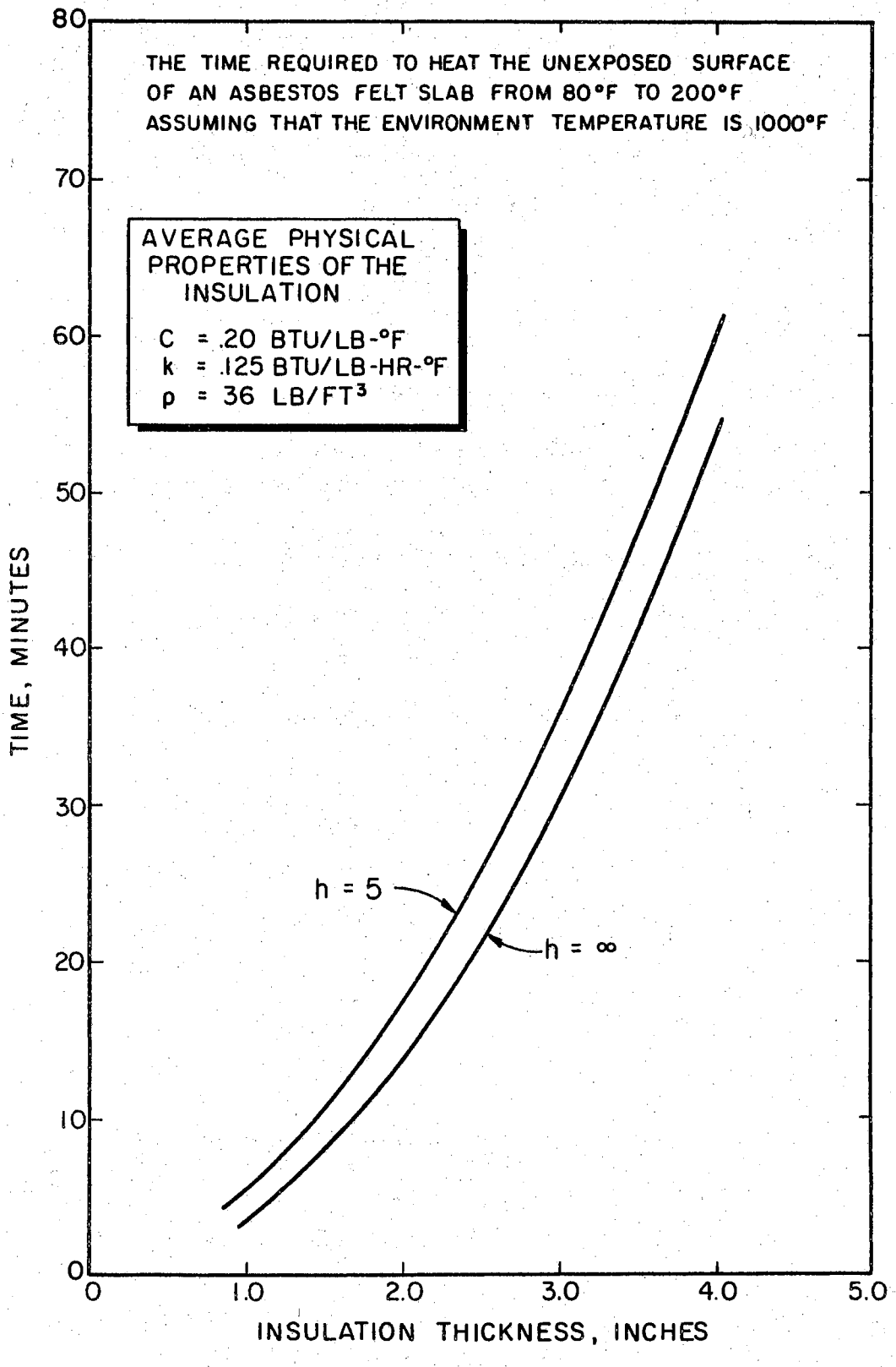

Figure 9. Flat Slab Insulation Thickness

marily a function of the thermal conductivity of the insulation.

The Boelter charts for solid cylinders were used to calculate the hollow cylinder insulation for Figure 8. This was justified by assuming that heat conduction in a thick hollow cylinder can be approximated by the heat conduction in a solid cylinder with the same overall dimensions. If the thermal conductivity of the insulation is low, the approximation appears to be valid. A further discussion of the problem is given in the appendix.

An instrument should be designed to have a high R_m/R_r value. This will usually insure large fusible rod length changes in an operating instrument. As an initial design, a 1/2 inch diameter fusible rod might be used with a 2 inch diameter by 1/8 inch thick aluminum disk. This design combination is suggested because it has a high R_m^2 to R_r^2 ratio, (16 to 1), and (refer to Figure 7) the efficiency of the exposed surface remains high even for relatively large heat-transfer coefficients.

The length of the fusible rod is dependent on the maximum heat which is presupposed to be absorbed on the exposed metal surface. This dimension is left to the individual designer. Charts such as Figure 10 may be constructed to aid in selecting the proper rod length. Figure 10 shows the amount of heat required to melt various lengths of a 1/2 inch diameter fusible rod. The heat is absorbed through a 2 inch diameter by 1/8 inch thick aluminum plate. Thermo-physical data for Figure 10 were taken from references (5, 11, 13, 14).

Various material may be used for the fusible rod. Materials which do not burn or decompose at or near their melting points would be the most desirable.

Additional qualitative information on how the heat was supplied to

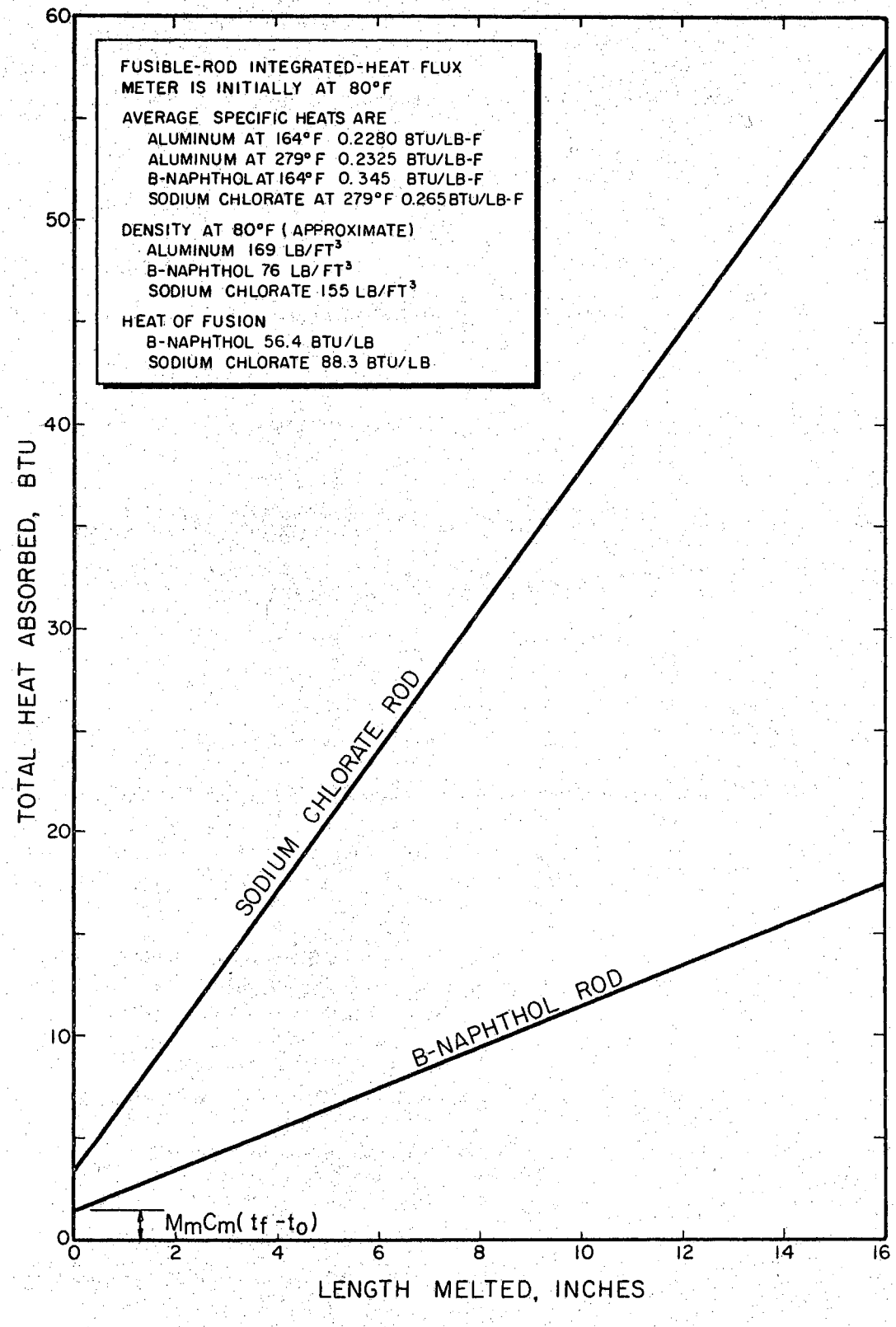

Figure 10. Heat Required to Melt a Given Length of Fusible-Rod

given surfaces could be obtained if several different fusible rods were used in the instruments. As an illustration, suppose that before a test two identical meters were placed near each other on the test grid. One of the meters contained a low-melting fusible rod while the other contained a high-melting fusible rod. After the test a large amount of the low-melting rod was found to have been consumed and none of the high-melting rod had been melted. This information tends to indicate that the temperatures around the two meters were relatively low during the test. If similar meter combinations are used throughout a test grid, it should be possible to map the relative hot and cold areas in the fire.

In conclusion, the fusible-rod integrated-heat flux meter should provide a simple means of measuring the heat output of a fire. It is rugged, inexpensive and easy to read and install.

Fusible-Rod Differential-Heat Flux Meter

Data on the heat flux and temperature transients in a fire could be very useful. The information would enable one to determine the progress and nature of the fire at any given moment. Unfortunately electronic instruments and recording devices are usually required to obtain this transient data.

One possible alternative to the use of electronic gear for measuring the heat flux transient is shown in Figure 11. The instrument is very similar to the fusible-rod integrated-heat flux meter in both design and operation. The only major difference between the two instruments is the recording device contained in the differential-heat flux meter. The recorder is a rotating drum and pen arrangement. The drum is slowly turned by means of a clock mechanism. As heat is absorbed by

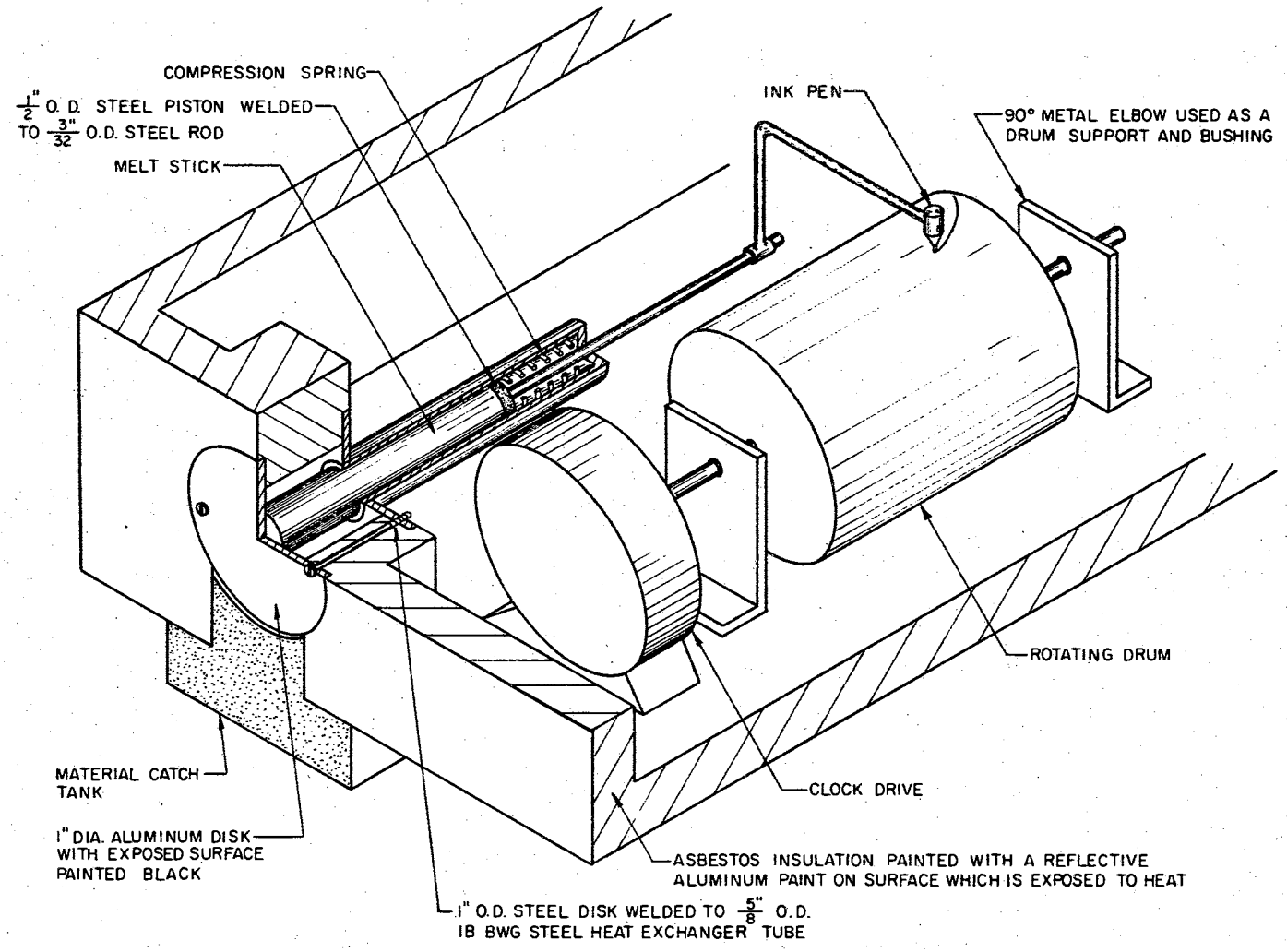

Figure 11. Fusible-Rod Differential-Heat Flux Meter

the exposed metal disk it is conducted to the fusible rod. The fusible rod melts and moves the ink pen across the turning drum. Thus a permanent record of the change in length of the fusible rod with time is obtained. This curve along with a simple mathematical expression may be used to calculate the heat flux to the exposed metal surface at any time during the melting period of the fusible rod.

Once the tip of the fusible rod has been heated to t_f, the additional heat which must be supplied to melt a small length dx of the rod is

$$dQ = \pi R_r^2 \rho_r \left[C_r(t_f - t_o) + \lambda_f \right] dx \tag{29}$$

Here the specific heat is evaluated at the average temperature between t_o and t_f. The density is evaluated at the temperature at which the dimensions of the fusible rod are measured (usually t_o).

Since the change in length of the fusible rod is known as a function of time, a change of variables may be made in equation 29. The result is

$$dQ = \pi R_r^2 \rho_r \left[C_r(t_f - t_o) + \lambda_f \right] \frac{dx}{d\theta} \, d\theta \tag{30}$$

The average heat flux on the exposed metal surface may be calculated by dividing equation 30 by $\pi R_m^2 d\theta$. Therefore,

$$q = \frac{R_r^2 \rho_r}{R_m^2} \left[C_r(t_f - t_o) + \lambda_f \right] \frac{dx}{d\theta} \tag{31}$$

Some radial temperature gradients will exist in the exposed metal surface. Therefore the instrument will not be as efficient as an "ideal" device (an instrument with no temperature gradients in the exposed metal

surface.) If the average heat-transfer coefficient can be estimated, the heat absorbed by an "ideal" instrument can be calculated from equation 32. The heat absorption efficiency η_A is calculated from equation 25.

$$q = \frac{R_r^2 \rho_r}{\eta_A R_m^2} \left[C_r (t_f - t_o) + \lambda_f \right] \frac{dx}{d\theta} \tag{32}$$

The derivative $dx/d\theta$ in equation 32 may be evaluated from the change in rod length plot by any one of several numerical differention techniques. As an illustration, consider the following example.

Example 4. A typical change in rod length versus time plot is shown in Figure 12. With the aid of this figure, graph the heat flux to the exposed surface as a function of time. The exposed metal is a 2 inch diameter by 1/8 inch thick aluminum disk. The 1/2 inch diameter fusible rod is made from β-naphthol. Assume that the efficiency of the exposed metal surface is 1.

Given:

C_r	0.345 BTU/lb-F
t_f	249 F
t_o	80 F
λ_f	56.4 BTU/lb
ρ_m	169 lb/ft^3
ρ_r	76 lb/ft^3

The derivatives $dx/d\theta$ are now calculated at various times. Several numerical procedures for evaluating the derivatives of a tabulated function are presented by Southworth and Deleeuw (19). Basically the procedures involve fitting a polynomial to several of the tabulated points.

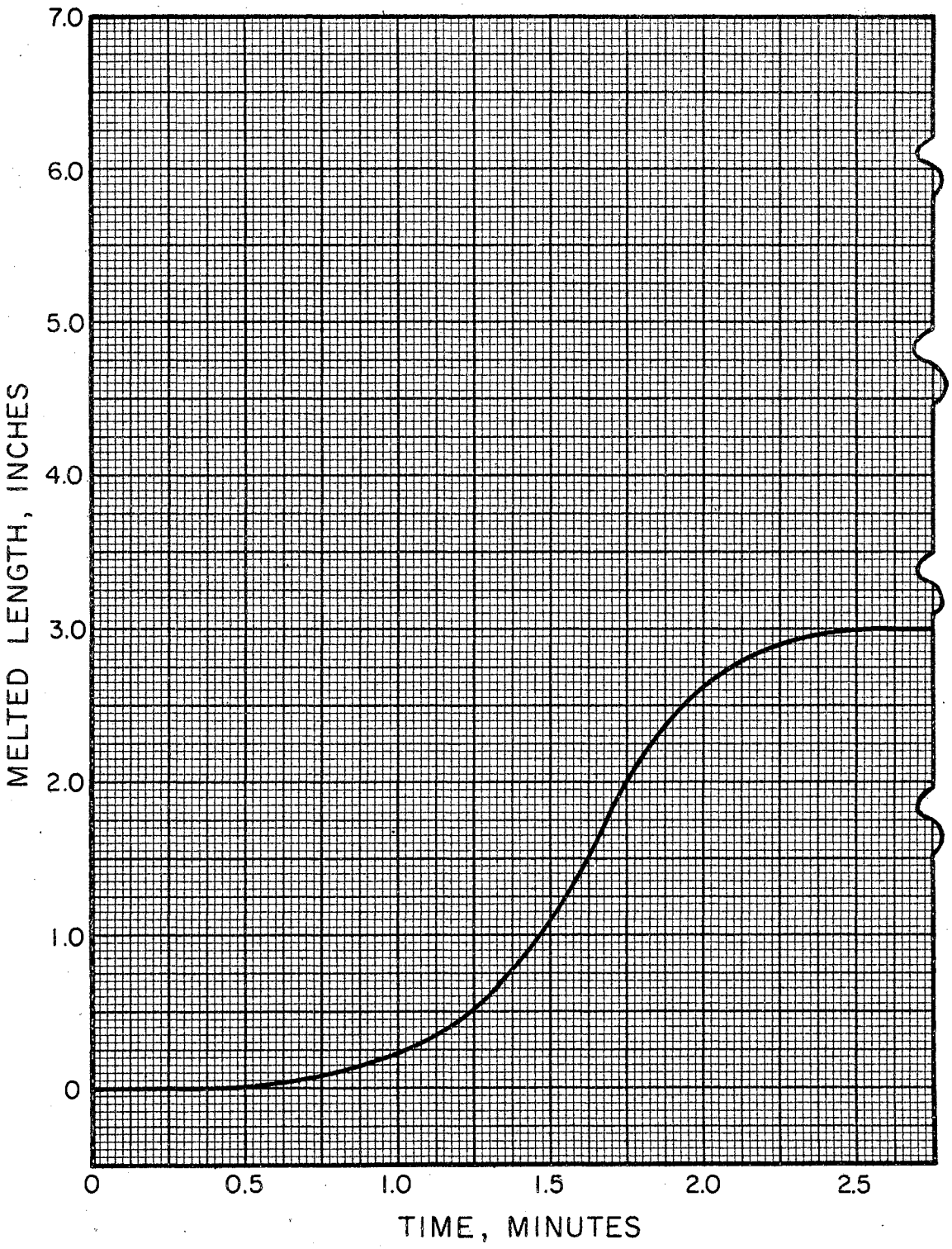

Figure 12. Example Plot of Rod Length vs. Exposure Time

The derivative of this polynomial is then used to represent the derivative of the tabulated function. If one chooses to evaluate the derivatives of the function at equally spaced abscissae, the difficulty of the calculations is greatly reduced.

The following expression for equally spaced abscissae was used to calculate the derivatives which are listed in Table I.

The derivative at point z_3 is

$$\frac{dy}{dz} = \frac{-y_5 + 8y_4 - 8y_2 + y_1}{12\Delta z} \tag{33}$$

Here z denotes the independent variable and y denotes the dependent variable. The incremental change in z is Δz. Equation 33 was derived from considerations of the central differences about a point z (19).

TABLE I

RESULTS OF HEAT FLUX CALCULATION

Time (min)	Length Melted (in)	$dx/d\theta$ (ft/hr)	Heat Flux (BTU/ft^2-hr)
0.250	0.000		
0.375	0.000		
0.500	0.000	.416	227
0.625	0.025	1.50	816
0.750	0.075	2.50	1360
0.875	0.150	3.58	1950
1.000	0.250	3.78	2060
1.125	0.350	5.65	3070
1.250	0.540	8.50	4620
1.375	0.775	11.01	5990
1.500	1.100	15.12	8230
1.625	1.525	18.65	10100
1.750	2.000	17.70	9630
1.875	2.380	12.55	6830
2.000	2.630	8.20	4460
2.125	2.800	5.27	2860
2.250	2.900	3.04	1650
2.375	2.960	2.00	1090
2.500	3.000	0.734	399
2.625	3.000		
2.750	3.000		

Small time increments were taken to insure that the data shown in Table I reflected the actual slope changes in the rod length plot.

Equation 32 was used to calculate the heat fluxes to the exposed metal surface. These fluxes are shown as a function of time in Figure 13. After examining Figures 12 and 13 it appears that the heat flux is initially very low; that it increases to a maximum and then decreases again to a low value.

The values for the heat fluxes shown in Figure 13 are not highly accurate. Small errors in the tabulated function can be greatly magnified when the $dx/d\theta$ derivative is evaluated. Errors in the value of the derivative of an order of magnitude or larger may be common. If the change in rod length plot can be accurately read, then the errors in the tabulated data can be reduced. This can be done by increasing the scales of the ordinate and abscissa. The ordinate can be increased by increasing the exposed surface area to fusible rod cross-sectional area ratio of an instrument. Therefore, if two similar instruments are exposed to the same fire environment, the instrument with the largest area ratio will record the largest rod length change.

The time scale can be increased by simply increasing the circumferential velocity of the drum. An acceptable time scale might be 1/2 minute per inch. Each rotation of the drum can be considered as an extension of the time scale. Plots similar to Figure 14 may be obtained. Figure 14 shows that the recording drum revolved almost three times during the melting period for the fusible rod. In this 7.5 minute period about 4.6 inches of the fusible rod were melted. The dotted lines indicate the continuation of the time scale.

The insulation problems associated with this instrument are similar to the ones associated with the fusible-rod integrated-heat flux meter.

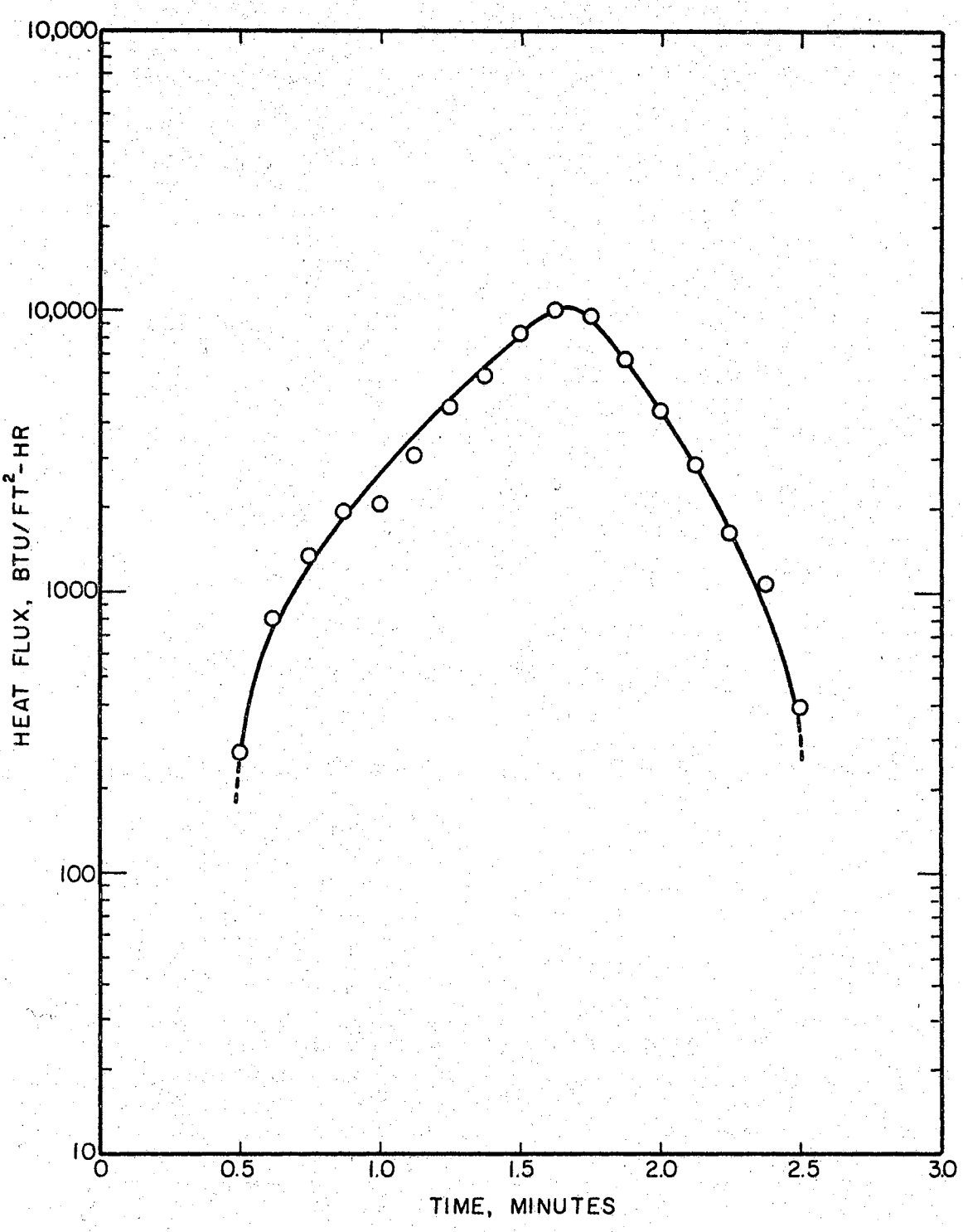

Figure 13. Heat Flux Versus Time Curve

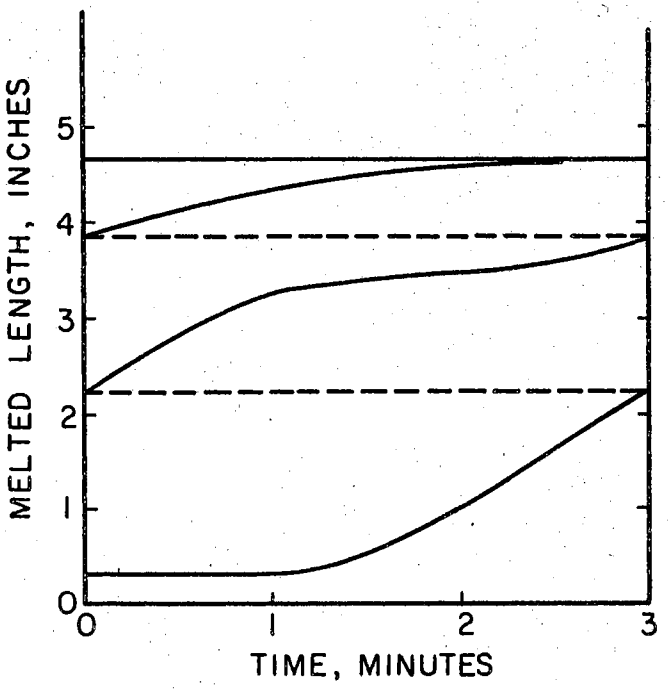

Figure 14. Extended Rod Length vs. Exposure Time Plot

Some general criteria for the maximum allowable amount of heat conducted through the insulation must be decided upon. Charts similar to Figure 9 can then be constructed. These charts will enable one to decide upon the amount of insulation required to keep the instrument cool.

Most of the materials required for constructing this instrument are readily available. The rotating drum can be made from sheet metal or an ordinary tall fruit juice can. Obtaining a suitable drive mechanism for the drum may be a problem. If an alarm clock mechanism is used, it will need to be altered so that an acceptable drum speed can be maintained. Other possible driving mechanisms might include war surplus fuse timing devices and mechanically or battery-driven gear trains from model cars and toys.

Complexity and cost are the major disadvantages of this instrument. In theory the makeshift recorder may be easily constructed and operated;

in actual practice this may not be true. The cost of materials and fabrication may exceed the $10 per unit maximum recommended in Chapter II. Despite these limitations, the instrument may prove to be a practical means of measuring the heat flux transient in a fire.

Evaporative Dosimeter

The evaporation of a liquid may be used as the basis for the design of instrument which measure the total heat absorbed by a surface. A conceptual drawing of such an instrument is shown in Figure 15. The instrument is fundamentally a vented liquid container. Initially the devices are filled with a known amount of liquid before being exposed to a test fire. After the test the instruments are retrieved and the amount of liquid evaporated is measured. If some of the liquid was vaporized during the test, then the total amount of heat absorbed by the instrument can be calculated.

The filling of the dosimeter may be facilitated by the use of a calibrating plunger. First the cup is filled approximately to the brim with a suitable liquid. Then the plunger is inserted until the lower rod strikes the bottom of the cup. The plunger is removed and the quick turn cap is put in place. Thus, some of the liquid has been forced out of the container by the plunger but a known amount remains.

If A_m is the total exposed area of the dosimeter and θ is the exposure time, then the total heat transferred to the dosimeter during a test is

$$Q_t = hA_m \int_o^{\theta} (t_s - t_m) d\theta \qquad (34)$$

This amount of energy must be absorbed by the dosimeter and its contents.

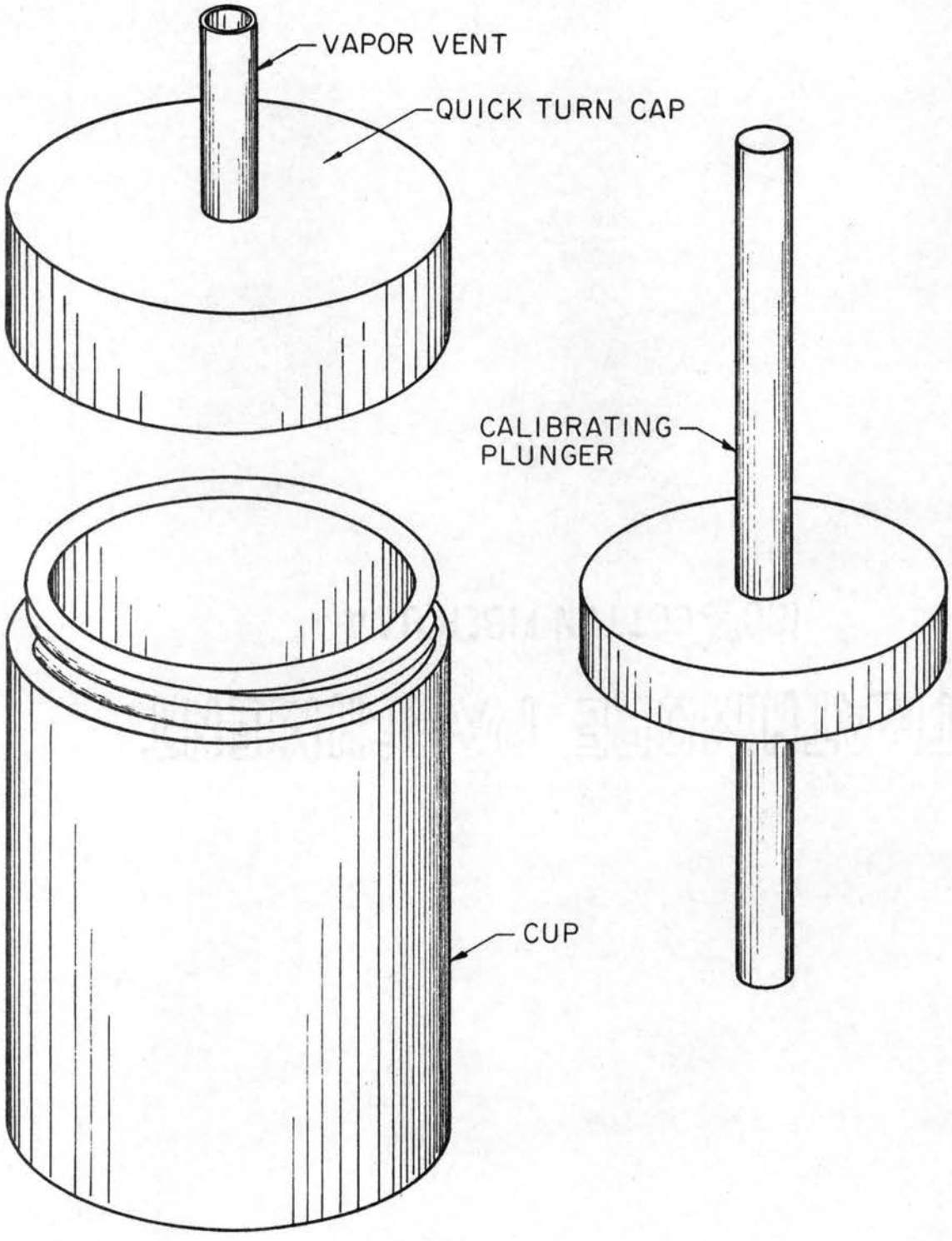

Figure 15. Evaporative Dosimeter

The sensible heat absorbed by the container and its contents when being heated from t_o to the boiling point of the liquid is

$$Q = \int_{t_o}^{t_b} (M_m C_m + M_{i\ell} C_\ell) dt \tag{35}$$

where M_m and $M_{i\ell}$ are the mass of the metal container and the initial mass of the liquid. If the specific heats C_m and C_ℓ are evaluated at the average temperature between t_o and t_b, equation 35 reduces to

$$Q = (M_m C_m + M_{i\ell} C_\ell)(t_b - t_o) \tag{36}$$

After the liquid in the dosimeter has been heated to its boiling point, any additional heat absorbed dQ will vaporize a mass dM of the test liquid.

$$dQ = -\lambda_b dM \tag{37}$$

If a mass M_b of the liquid is vaporized during a test, the total heat absorbed by the dosimeter is

$$Q_t = (M_m C_m + M_{i\ell} C_\ell)(t_b - t_o) + \lambda_b M_b \tag{38}$$

If the duration of the fire is known, then the average heat flux to the dosimeter is given by

$$q = \frac{Q_t}{A_m \theta} \tag{39}$$

Since the measured variable is M_b, the greatest precision in the value of Q_t can be obtained if $\lambda_b M_b >> (M_m C_m + M_{i\ell} C_\ell)(t_b - t_o)$. If the fire characteristics are known, this may be accomplished by proper selection of the test liquid and a reasonable mechanical design for the

dosimeter.

Charts similar to Figure 16 may aid in the selection of a suitable fluid and dosimeter design combination. Figure 16 shows the relation between the amount of fluid vaporized in a specific instrument and the total amount of heat absorbed. The vaporization efficiency η_v is defined as the ratio of the heat absorbed, which causes a measurable loss of liquid, to the total heat absorbed.

$$\eta_v = \frac{\lambda_b M_b}{(M_m C_m + M_{i\ell} C_\ell)(t_b - t_o) + \lambda_b M_b} \tag{40}$$

The specific heats C_m and $C_{i\ell}$ are again evaluated at the average temperature between t_o and t_b. The thermal property data required for the construction of Figure 16 was taken from references (5, 6, 7, 8, 12).

The liquids considered in Figure 16 may be divided into high boiling and low boiling liquids. Water, chloroform and carbon tetrachloride make up the low boiling group while ethylene glycol and 1,2-propylene glycol make up the high boiling group. If a dosimeter is to measure the total heat absorbed by a low temperature surface ($100^{\circ}F$ to $250^{\circ}F$), then, of the three low boiling liquids, water seems to be the logical choice for a working fluid. When choosing between various working fluids, one should also consider the amount of heat which the instrument may be exposed to. For the given dosimeter the energy required to vaporize 6.1 cubic inches (100 ml) of water is about 250 BTU, while the energy required to vaporize an equal volume of chloroform or carbon tetrachloride is only about 40 BTU. Under certain conditions, such as a short exposure time, a water-filled dosimeter might not register any loss of liquid, but a dosimeter filled with either chloroform or carbon tetrachloride might register a substantial liquid loss. In

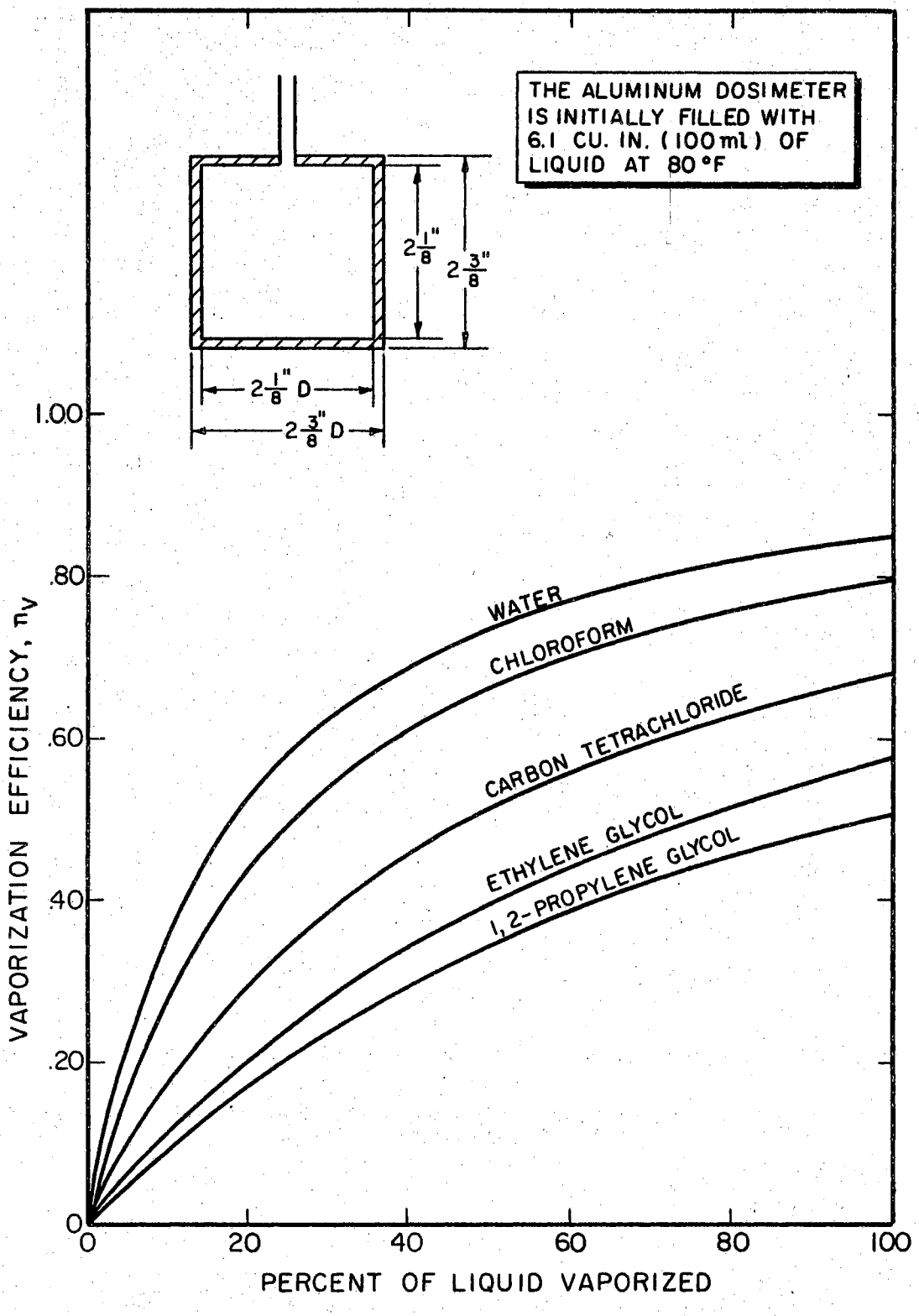

Figure 16. The Capacity of an Instrument to Use Absorbed Heat to Vaporize a Liquid

this case either chloroform or carbon tetrachloride would be a better choice than water for the working fluid. Since the efficiency is higher for chloroform than for carbon tetrachloride, chloroform would be the best choice of the two liquids.

Ethylene glycol or 1,2-propylene glycol might be considered as working fluids if information on the amount of energy absorbed from a fire by a surface at 350 F to 400 F is to be obtained. For the given dosimeter design, the approximate amounts of heat required to vaporize 6.1 cubic inches of ethylene glycol or 1,2-propylene glycol are 160 BTU and 140 BTU respectively. Thus, the total amounts of heat which can be registered by instruments filled with either of the two liquids are comparable in magnitude. Since the efficiencies for an ethylene glycol-filled instrument are higher than the corresponding efficiencies for a 1,2-propylene glycol-filled instrument, ethylene glycol would be the best choice for the working fluid.

One possible way to increase the efficiencies for a given volume of liquid is to reduce the mass of the dosimeter. This may be done by decreasing the wall thickness, but too thin a wall can reduce the ability of a dosimeter to absorb available heat. Once the liquid has started to boil, the surfaces of the dosimeter below the liquid level remain near the boiling temperature. Those surfaces which are above the liquid level are heated to a somewhat higher temperature. If the dosimeter has thin walls, then the temperature gradients in the portion above the liquid level will be steep. Thick walls tend to lessen the magnitudes of the temperature gradients. The wall thickness should be thin enough to assure a small sensible heat for the metal, but thick enough to insure that large temperature gradients do not build up in the metal.

In order to determine what mechanical designs for the dosimeter would be the most effective, a heat absorption efficiency is defined. The heat absorption efficiency is the ratio of the total heat absorbed by the dosimeter, after the working fluid has been heated to its boiling point t_b, to the total heat which would be absorbed by the dosimeter if the entire exposed surface were at t_b. The efficiency may be written as

$$\eta_a = \frac{\int_o^{A_m} (t_s - t_m) dA}{(t_s - t_b) A_m} \tag{41}$$

The temperature distribution over the surface of the dosimeter must be calculated before equation 41 can be integrated. For convenience the dosimeter is divided into three domains as shown in Figure 17. Neglecting temperature gradients across the thickness, the temperature distribution is assumed to be one-dimensional, axial in the second domain and radial in the third domain. The first domain is assumed to be 100 per cent efficient because it is below the liquid level.

In the following derivations it will be assumed that the heat-transfer coefficient is constant over the entire surface and that the physical properties of the dosimeter material are independent of temperature. The steady state heat conduction equations for the second and third domains may be written as

$$\frac{d^2 \nu_2}{dx^2} - m^2 \nu_2 = 0 \qquad \text{Second Domain} \tag{42}$$

$$\frac{d^2 \nu_3}{dr^2} + \frac{1}{r} \frac{d\nu_3}{dr} - n^2 \nu_3 = 0 \qquad \text{Third Domain} \tag{43}$$

where

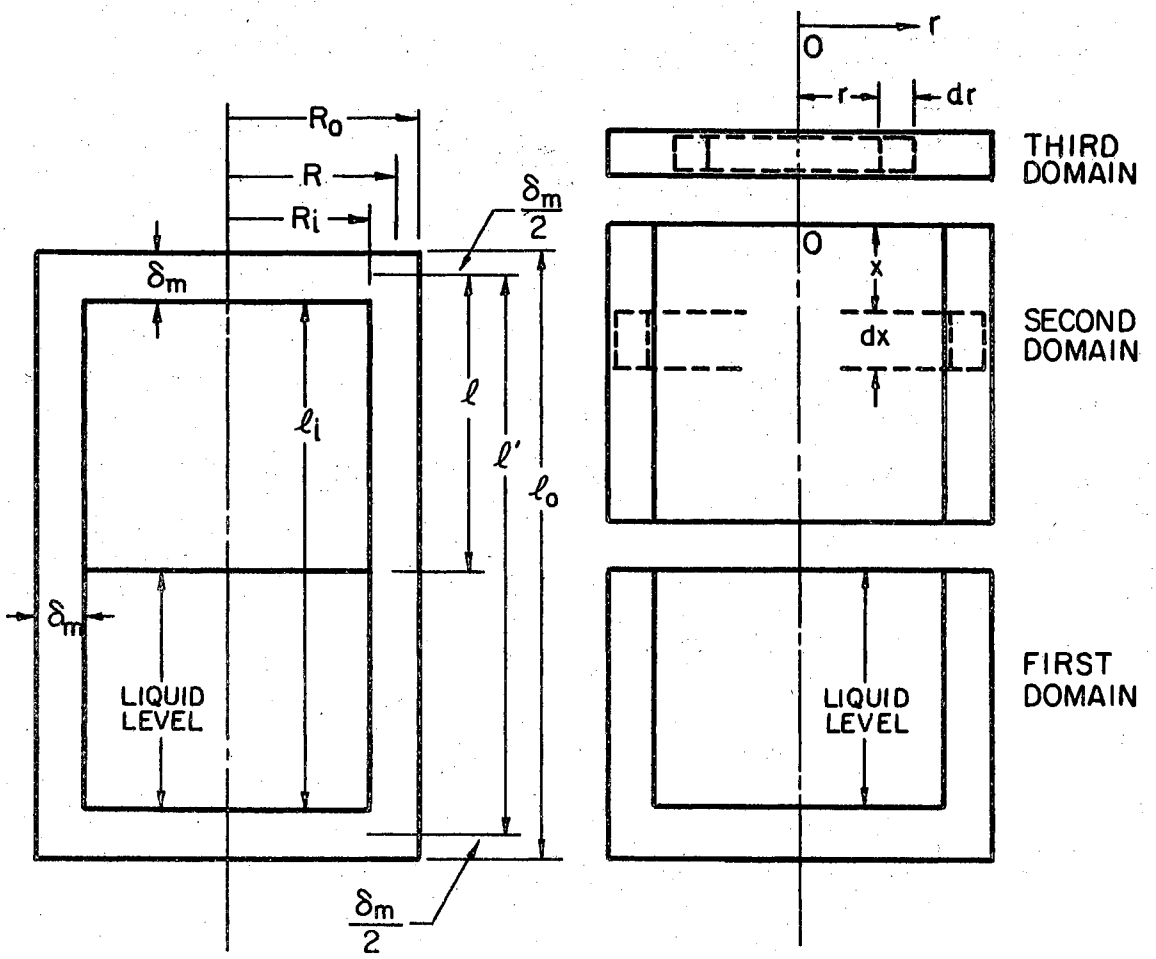

Figure 17. Schematic of Evaporative Dosimeter with Temperature Domains

$$\nu_2 = t_s - t_{m,2} \tag{44}$$

$$\nu_3 = t_s - t_{m,3} \tag{45}$$

$$m = \sqrt{2hR_o/(k_m(R_o^2 - R_i^2))} \tag{46}$$

$$n = \sqrt{h/k_m \delta_m} \tag{47}$$

The subscripted temperatures $t_{m,2}$ and $t_{m,3}$ denote the metal temperatures in the second and third domains respectively.

Equation 42 is an ordinary linear homogeneous differential equation with constant coefficients. Its solution is

$$\nu_2 = C_1 \cosh(mx) + C_2 \sinh(mx) \tag{48}$$

Equation 43 is a form of Bessel's equation. The standard solution for this equation is

$$\nu_3 = C_3 I_o(nr) + C_4 K_o(nr) \tag{49}$$

The arbitrary constants C_1, C_2, C_3, and C_4 are evaluated by applying the following boundary conditions:

(1) $\nu_2 = t_s - t_b = \nu_o$ at $x = \ell$

(2) $\nu_2 = \nu_3$ at $x = 0$, $r = R$

(3) $\dfrac{d\nu_3}{dr} = 0$ at $r = 0$

(4) $\dfrac{d\nu_2}{dx} = \dfrac{d\nu_3}{dr}$ at $x = 0$, $r = R$

The constants are

$$C_1 = \frac{\nu_o m I_o(nR)}{m I_o(nR)\cosh(m\ell) + n I_1(nR)\sinh(m\ell)} \tag{50}$$

$$C_2 = \frac{\nu_o n I_1(nR)}{m I_o(nR)\cosh(m\ell) + n I_1(nR)\sinh(m\ell)} \tag{51}$$

$$C_3 = \frac{\nu_o m}{m I_o(nR)\cosh(m\ell) + n I_1(nR)\sinh(m\ell)} \tag{52}$$

$$C_4 = 0 \tag{53}$$

The heat absorption efficiency of the dosimeter may now be calculated from equation 41. The integral of equation 41 is broken into four parts.

$$\eta a = \left[C_3 \int_o^R I_o(nr) r \, dr + R_o \int_o^{\ell} (C_1 \cosh(mx) + C_2 \sinh(mx) dx + R_o \nu_o \int_{\ell}^{\ell'} dx + \nu_o \int_o^R r \, dr \right] / \left[\nu_o (R^2 + R_o(\ell')) \right] \tag{54}$$

Equation 54 is integrated and reduced to

$$\eta a = \left[R_o n (C_5 \sinh(m\ell) + C_6(\cosh(m\ell) - 1)) + RmC_7 I_1(nR) + \right.$$

$$mn(R_o(\ell'-\ell) + R^2/2)\Big] \Big/ \Big[mn(R^2 + R_o(\ell'))\Big] \tag{55}$$

where $C_5 = C_1/\nu_o$ (56)

$C_6 = C_2/\nu_o$ (57)

$C_7 = C_3/\nu_o$ (58)

There are no temperature terms in equation 55. Therefore, for any given dosimeter design the efficiency is only a function of the heat-transfer coefficient and the liquid level.

Figures 18, 19 and 20 were constructed to aid in the evaluation of different mechanical designs for the dosimeter. In each figure the heat absorption efficiency is plotted against the per cent of liquid vaporized with the over-all heat-transfer coefficient as a parameter. Each of the aluminum dosimeters, for which the figures were drawn, has a wall thickness of 1/8 inch and an approximate volume of 7.63 cubic inches (125 ml). Figure 18 shows the heat absorption efficiency for a cylindrical dosimeter which has a minumum surface to volume ratio. Figures 19 and 20 were drawn for dosimeters which have approximately twice the exposed area of the minimum area dosimeter of Figure 18. These figures show that for a given volume, wall thickness, heat-transfer coefficient and amount of liquid vaporized, the efficiency increases with a decrease in dosimeter height. Generally, squat dosimeters have high efficiencies.

A very short instrument, such as the one shown in Figure 19, may provide several practical problems. It may not be possible to accurately measure the initial liquid volume with a calibrating plunger. When the plunger is inserted into the cup, it should be vertical. If the plunger is tilted to the side or inserted rapidly, an error in the

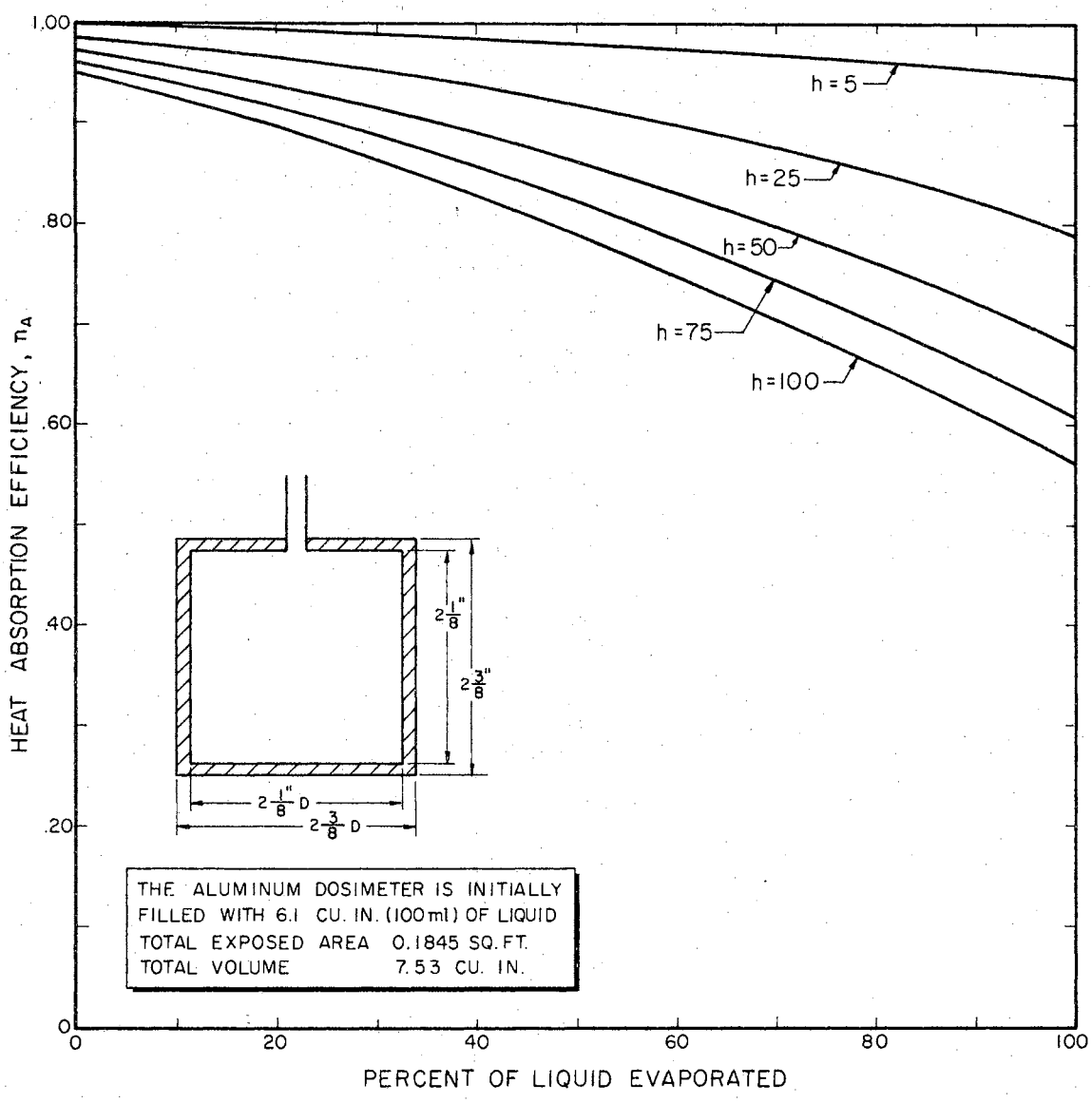

Figure 18. Heat Absorption Efficiency of Exposed Metal Surface

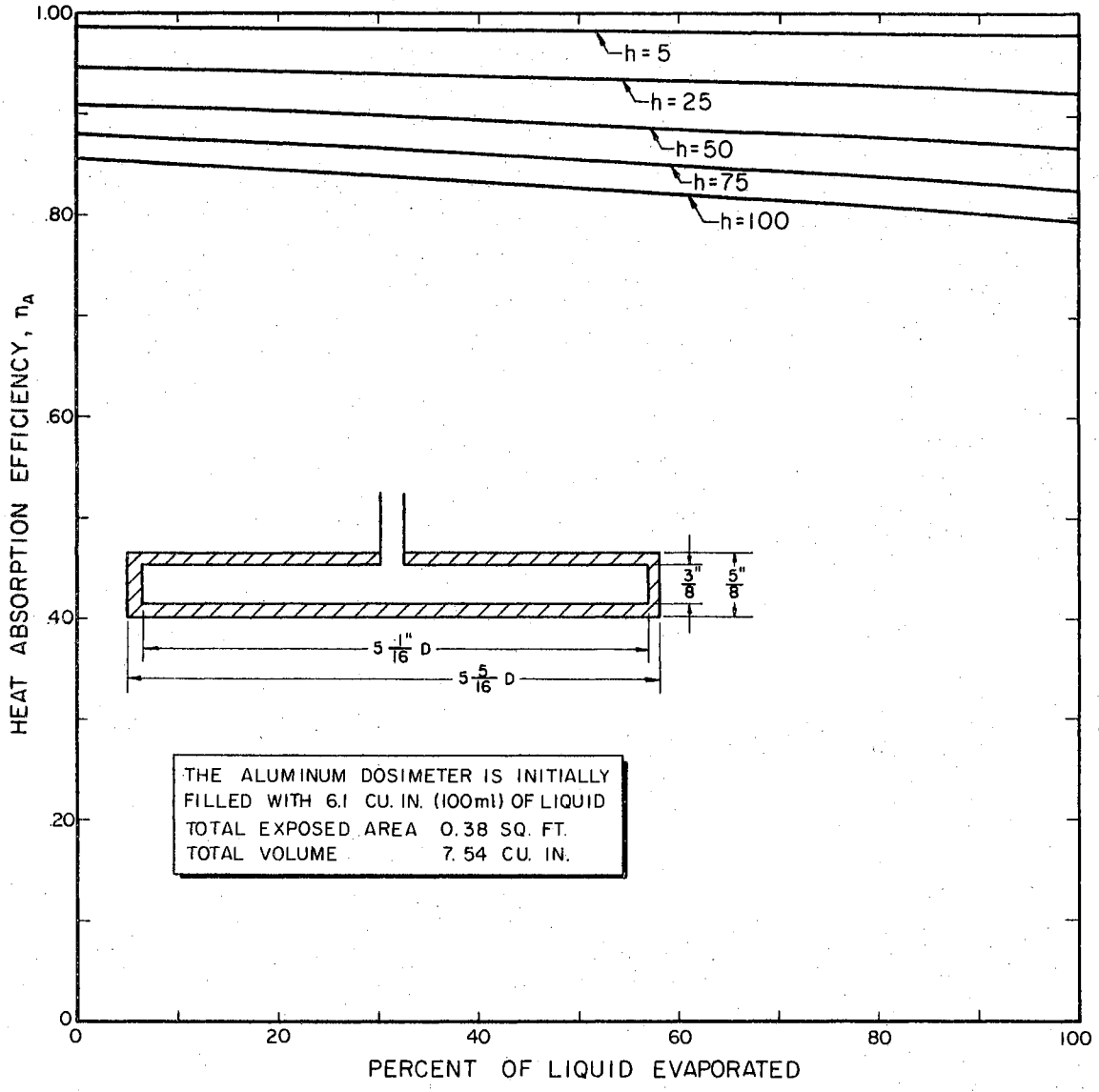

Figure 19. Heat Absorption Efficiency of Exposed Metal Surface

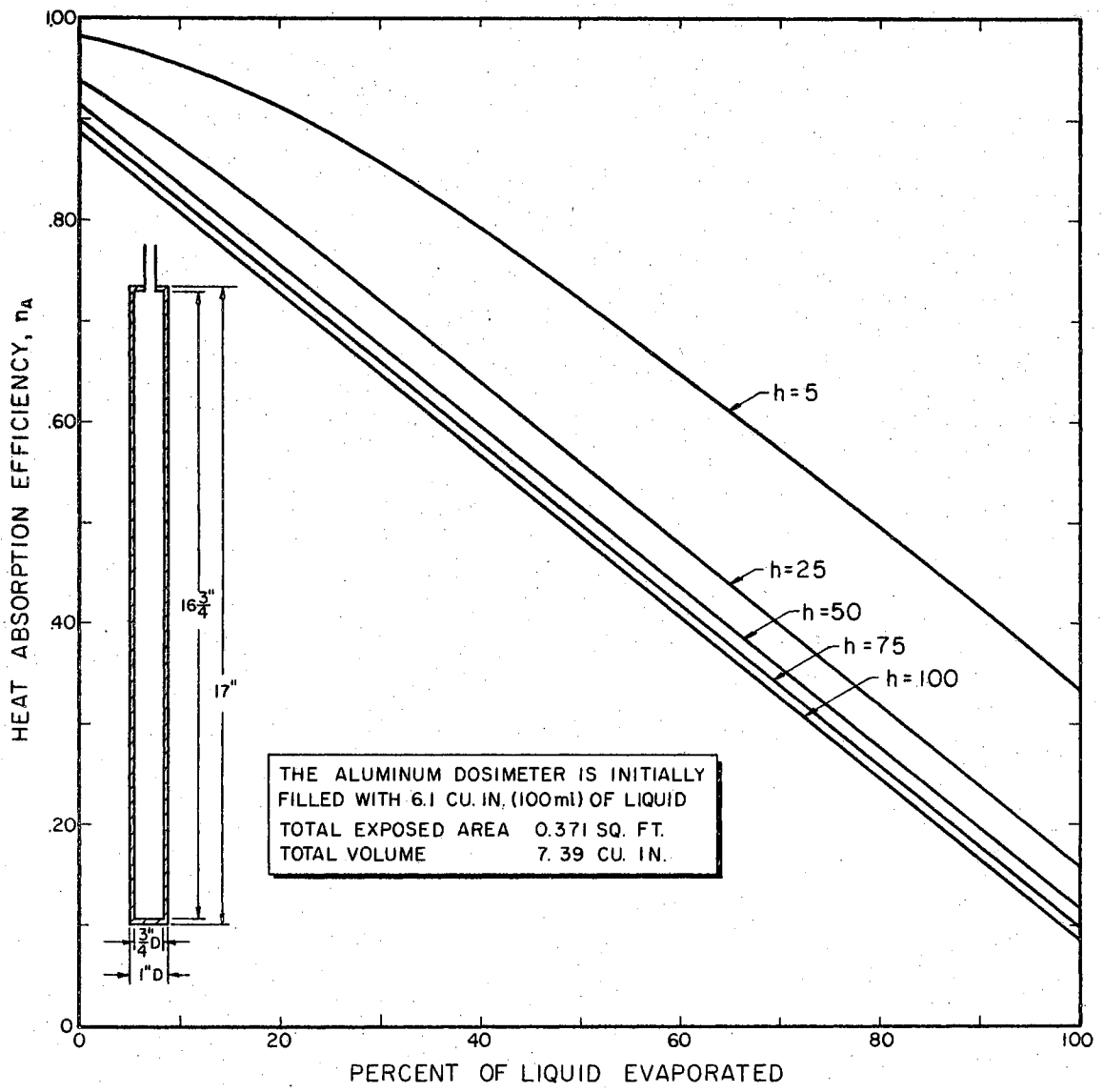

Figure 20. Heat Absorption Efficiency of Exposed Metal Surface

initial liquid volume may be made. This error will be most pronounced in a squat instrument. The error may be reduced by using a calibrated syringe instead of the plunger to measure the initial liquid volume.

A flat dosimeter design also increases the probability of liquid loss due to entrainment with the escaping vapors. Probably the best design is that of the approximately minimum area/volume ratio dosimeter; one with the height equal to its diameter. This is a compromise between the very long and the very short designs. It combines some of the best and worst attributes of both extremes. Initial liquid volumes can be easily measured with a calibrated plunger, and a relatively large space for vapor-liquid disengagement can be provided. However, the heat absorption efficiencies are not as high as the efficiencies for the short dosimeter design.

Liquid entrainment may occur when the dosimeter is exposed to a high heat flux. Some of the liquid, in the form of small drops, may be carried through the vapor vent with the escaping vapors. This will cause the dosimeter to register too high a liquid loss. As a means of reducing the entrainment, a small metal baffle may be placed just below the inside opening to the vapor vent. This will help to knock the liquid out of the escaping vapors.

Example 5. An aluminum evaporative dosimeter, which is identical to the one for which Figure 18 was drawn, was filled with 6.1 cubic inches (100 ml) of water at 80 F. The dosimeter was then exposed in a test fire. After the test it was found that 1.83 cubic inches (30 ml) of water had been vaporized. Infrared photography was used to map the fire. The films show that the area in which the dosimeter was placed was completely engulfed by the flames for a period of 5 minutes. Cal-

culate (a) the total heat absorbed by the dosimeter and (b) by assuming that the heat was absorbed during the 5 minute period in which the dosimeter was completely surrounded by the flames, calculate the average heat flux to the dosimeter.

Given:

C_ℓ	1.0 BTU/lb-F
C_m	0.227 BTU/lb-F
ℓ_i	2.125 in.
ℓ_o	2.375 in.
R_i	1.063 in.
R_o	1.188 in.
t_b	212 F
t_o	80 R
λ_b	970 BTU/lb
ρ_ℓ	62.18 lb/ft^3
ρ_m	169 lb/ft^3
θ	5 min

The physical properties for aluminum and water were taken from references (5, 12). Densities were evaluated at the temperature at which the dimensions of the dosimeter were measured (80^{o}F) and the specific heats were evaluated at the average temperature between t_o and t_b.

(a) The mass terms in equation 38 are calculated from the following equations:

$$M_m = \pi\rho_m \left[R_o^2 \ell_o - R_i^2 \ell_i\right] = .292 \text{ lb} \tag{59}$$

$$M_{i\ell} = V_{i\ell}\rho_\ell = .220 \text{ lb} \tag{60}$$

$$M_b = V_b \rho_\ell = .0659 \text{ lb} \tag{61}$$

The total measurable heat absorbed by the dosimeter is calculated from equation 38, giving 102 BTU.

(b) If

$$A_m = 2\pi \left[R_o^2 + R_o \ell_o \right] \tag{62}$$

then the average heat flux to the metal surface is calculated from equation 39. Thus,

$$q = 6640 \text{ BTU/ft}^2\text{-hr}$$

This is probably a relatively high heat flux for most fires. A dosimeter filled with chloroform instead of water (at the same initial conditions) would have required an average heat flux of only 1240 BTU/ft^2-hr for the five minute heating period to vaporize the same volume of liquid. The additional data for the chloroform case are

$$C_\ell = 0.2350 \text{ BTU/lb-}^\circ\text{F}$$
$$C_m = 0.2255 \text{ BTU/lb-}^\circ\text{F}$$
$$t_b = 142 \ ^\circ\text{F}$$
$$\lambda_b = 107 \text{ BTU/lb}$$
$$\rho_\ell = 91 \text{ lb/ft}^3$$

The evaporative dosimeter, like the fusible-rod integrated-heat flux meter, may be used to map the relatively hot and cold areas in a fire (see previous discussion on page 39). By using several different liquids in identical meters, it should be possible to obtain qualitative information on the heat absorbed by surfaces which are at various temperatures throughout a fire.

Almost any liquid which has a boiling point may be used in the dosimeter. If flammable liquids are used, care should be taken to flare the vapors at some distance from the dosimeter. This can be done by using a long thin tube for the vapor vent.

The dosimeter should be constructed from a material which has a high thermal conductivity. The high thermal conductivity will help to insure that only small temperature gradients exist in the walls of the meter. Because of its high thermal conductivity, availability and cheapness, aluminum is suggested as being the most ideal material for construction.

The evaporative dosimeter should provide a simple means of measuring the total heat absorbed by a surface in a fire environment and the average heat flux. If different liquids are used in the dosimeters, then some additional information on the relative hot and cold areas in a fire can be obtained.

Heat Switch

A simple heat sensing device is illustrated in Figure 21. It consists essentially of a thin aluminum plate on which wafers of various heat-sensitive materials are supported. The heat-sensitive wafers are held in place by spring-loaded electrical contacts. A self-contained recorder is connected to the aluminum plate and the entire device, except for an exposed surface of the aluminum plate, is enclosed in an insulated housing.

When the device is exposed to a fire environment, heat is conducted through the aluminum plate to the heat-sensitive wafers and causes them to melt. As the thin wafers melt, the spring-loaded contacts complete

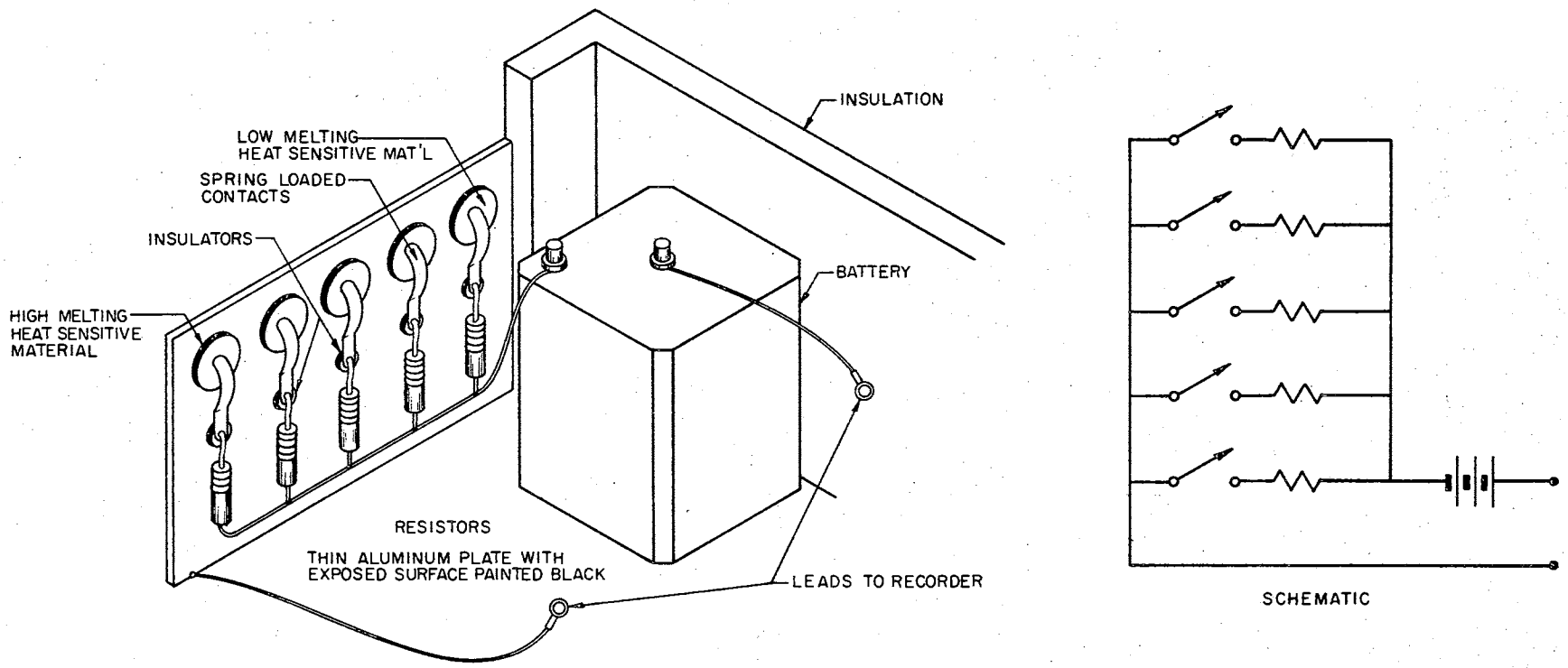

Figure 21. Temperature Sensing Switch

circuits by coming in contact with the aluminum plate. A resistor cascade is provided to increase the current to the recorder as each circuit is closed. Thus, a series of successively increasing step current impulses is sent to the recorder. In this manner, a temperature versus time record is obtained for the aluminum plate.

Since the aluminum plate is thin and has a large thermal conductivity, the flow of heat to or from the plate is primarily controlled by the convective resistance. Therefore, the temperature may be assumed to be uniform throughout the plate and a function of time only. The incident net heat flux to the plate is equal to

$$q = C_m \rho_m \delta_m \frac{dt_m}{d\theta} \tag{63}$$

Equation 63 may be evaluated if the various derivatives $dt_m/d\theta$ are calculated from a smoothed curve through the experimental output. In practice, the need to differentiate the experimental data may introduce large errors in the calculated heat flux.

The heat switch has a number of obvious limitations inherent in its design. There is a limit to the number of heat-sensing circuits which can be accommodated by the device. Once these circuits are closed they must remain closed for the duration of the test. Thus if an instrument is strongly heated during a test, all the circuits may be closed in rapid succession. The device would, therefore, be operative for only a short time. A very limited amount of information on the heat fluxes would be obtained.

When the aluminum plate has reached the melting temperature of one of the heat-sensitive wafers, there will be some time delay before the heat-sensitive wafer melts. The latent heat of fusion must be absorbed

by the wafer before it can melt. This is probably not too serious a problem. If the wafer is thin, only a small amount of heat will need to be absorbed; the time delay will be short.

Most of the materials required for the construction of the heat switch can be easily obtained. The spring loaded electrical contacts may be made from bent strips of spring steel. Cross-sections cut from "Tempilstiks" can be used as heat sensitive wafers. Obtaining a simple, cheap recorder for the instrument may be a problem. Perhaps, an ammeter mechanism with an attached ink pen could be used in conjunction with a rotating paper drum as a recorder. The use of commercially available battery-operated current recorders is not recommended because of their expense. Such recorders may be obtained from the Rustrak Instrument Company for about $100 each.

The heat switch may theoretically be used to obtain information on the heat flux transients in a flame. It is a simple and relatively rugged device. However, since no simple, cheap current recorder has been suggested, the heat switch does not at this time appear to be attractive.

Gas-Filled Temperature Probe

Another proposal was that the temperature transients in a fire might be measured with the aid of a gas-filled thin-walled metal container. The proposed instrument is illustrated by Figure 22. A known volume and hence mass of a gas are confined in the container. A pressure recorder is connected to the container by a capillary tube. The simple pressure recorder, as shown in Figure 22, consists of a Bourdon tube mechanism, an ink pen and a rotating paper drum. Any suitable mechanical

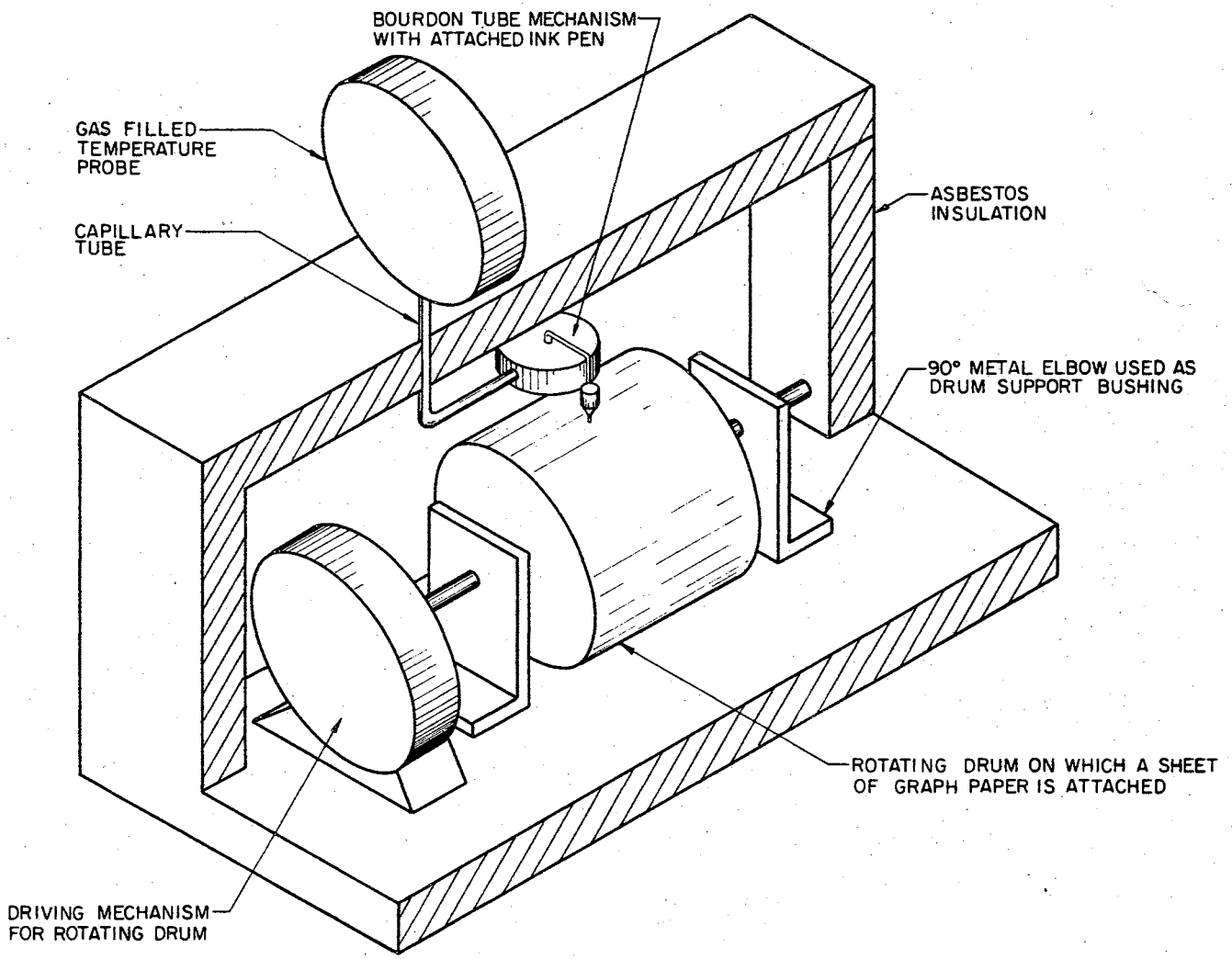

Figure 22. Gas-Filled Temperature Probe and Recorder

device, such as a clock mechanism, may be used to turn the drum.

During a test, the temperature probe is exposed to the fire environment. The confined gas is heated and causes the Bourdon tube mechanism to register the internal pressure of the confined gas on the rotating drum. Since the mass, volume and pressure of the gas are known, the temperature of the confined gas can be calculated from the ideal-gas law.

If the device is to effectively monitor the temperature transient in a fire, it should rapidly register the surrounding temperature. As a means of determining the feasibility of the temperature probe, the instrument's response to a simple step change in the temperature of the surroundings will be considered. The probe is assumed to be initially at the ambient temperature t_o. Suddenly the environmental temperature is raised to t_s and remains at that value. After the step change in the environmental temperature has occurred, the total heat transferred to the probe in time increment $d\theta$ is

$$dQ_t = hA_m(t_s - t_m)d\theta \tag{64}$$

This heat must be absorbed by the metal in the temperature probe and by the contained gas. The change in heat content of the metal is given by

$$dQ_m = M_m C_m dt_m \tag{65}$$

The change in heat content of the confined gas is

$$dQ_g = M_g C_g dt_g \tag{66}$$

Also

$$dQ_g = h'A'_m(t_m - t_g)d\theta \tag{67}$$

where h', A_m' and t_m' are the inside heat-transfer coefficient, the inside metal area and the inside metal temperature respectively. If the walls of the temperature probe are thin, $A_m' \approx A_m$ and $t_m' \approx t_m$. Hence equation 67 is rewritten as

$$dQ_g = h'A_m(t_m - t_g)d\theta \tag{68}$$

Two heat balances for the temperature probe are now written. Thus,

$$hA_m(t_s - t_m)d\theta = M_m C_m dt_m + h'A_m(t_m - t_g)d\theta \tag{69}$$

and

$$h'A_m(t_m - t_g)d\theta = M_g C_g dt_g \tag{70}$$

Equations 69 and 70 are rearranged and the following differential equations for t_m and t_g are obtained:

$$\frac{dt_m}{d\theta} + (a + b)t_m - bt_g = at_s \tag{71}$$

$$\frac{dt_g}{d\theta} + ct_g - ct_m = 0 \tag{72}$$

Now equations 71 and 72 are simultaneously solved together. The solutions are found to be

$$t_m = C_1 e^{(\beta+\omega)\theta} + C_2 e^{(\beta+\omega)\theta} + t_s \tag{73}$$

and

$$t_g = \frac{C_1 c}{\beta+\omega+c} e^{(\beta+\omega)\theta} + \frac{C_2 c}{\beta-\omega+c} e^{(\beta-\omega)\theta} + t_s \tag{74}$$

where $a = \dfrac{hA_m}{M_m C_m}$ (75)

$$b = \frac{h'A_m}{M_m C_m} \tag{76}$$

$$c = \frac{h'A_m}{M_g C_g} \tag{77}$$

$$\beta = -\left(\frac{a+b+c}{2}\right) \tag{78}$$

$$\omega = \frac{\sqrt{(a+b+c)^2 - 4ac}}{2} \tag{79}$$

The two arbitrary constants C_1 and C_2 are evaluated by applying the following boundary conditions to equations 73 and 74:

(1) $t_m = t_o$ at $\theta = 0$

(2) $t_g = t_o$ at $\theta = 0$

The constants are found to be

$$C_1 = \frac{(t_s - t_o)(\beta - \omega)(\beta + \omega + c)}{2\omega c} \tag{80}$$

and

$$C_2 = \frac{-(t_s - t_o)(\beta + \omega)(\beta - \omega + c)}{2\omega c} \tag{81}$$

Typical solutions of equations 73 and 74 are shown in Figure 23. The Figure shows the response characteristics of a typical temperature probe to a sudden change in the surrounding temperature with the external heat-transfer coefficient as a parameter. In all cases a low value of 1.0 BTU/ft^2-hr-F was assumed for the internal heat-transfer coefficient. It can be seen that the gas filled temperature probe is rather slow in registering a given change in the environmental temperature. This is particularly true when the external heat-transfer coefficient to the probe is low. The response characteristics of the probe can be

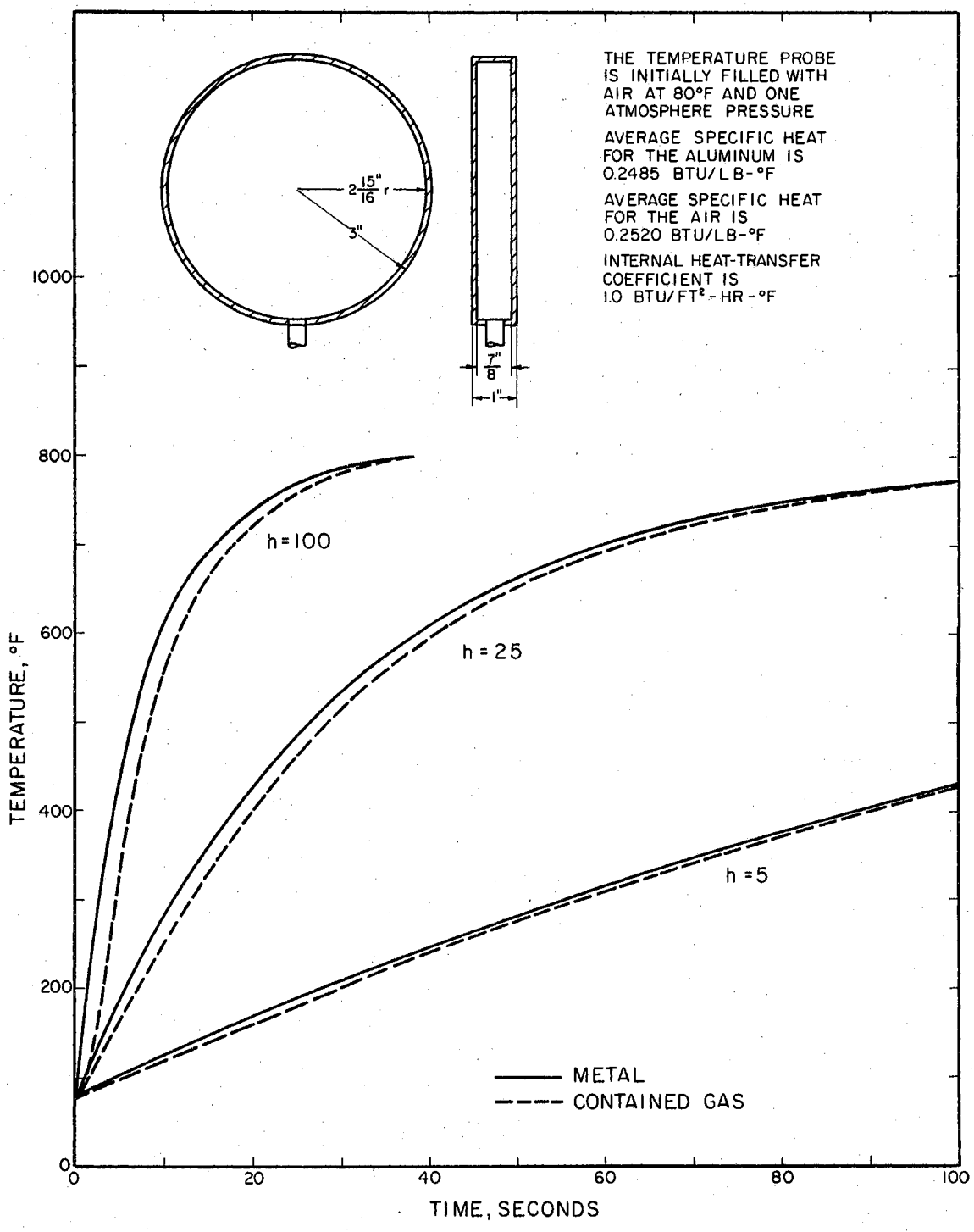

Figure 23. Temperature-Time History of a Gas Filled Temperature Probe Subjected to a Step Change in the Environmental Temperature

increased by decreasing the wall thickness of the probe; however, there is a limit to how thin the wall can be made. If the wall is too thin, the probe will be easily deformed as it is heated.

The addition of extended surface such as metal fins to the gas container does not appear to be a practical method of increasing the instrument's temperature response. The large amount of metal in the temperature probe is the main cause of the instrument's sluggishness. The added metal in the fins would tend to further decrease the response of the device to a temperature change.

In conclusion, the gas filled temperature probe does not appear to be suitable for monitoring temperature transients. It is too slow to accurately register the unsteady temperature changes in a fire.

CHAPTER VI

CONCLUSIONS AND RECOMMENDATIONS

This study has been primarily concerned with the design and mathematical evaluation of simple heat sensing devices for large fires. Various devices have been proposed. Some of the devices seem to be feasible; others appear to be unsuitable. A rather cursory description is given for those devices which seem unsuitable, while additional consideration is given to those devices which appear practical.

The following main conclusions were drawn from this study:

1. The maximum temperature indicator appears to be a suitable device for measuring the maximum temperature attained at any given point in a flame. Since the device operates with only a small temperature lag, it should indicate the true temperature of its immediate surroundings accurately.
2. The fusible-rod integrated-heat flux meter, fusible-rod differential-heat flux meter and the evaporative dosimeter all appear to be suitable devices for measuring the total heat absorbed by a surface in a fire.
3. Qualitative information may be obtained on the heat flux transients in a fire with the aid of the fusible-rod differential-heat flux meter. The device is somewhat unattractive because it requires a self-contained recorder.
4. The heat switch appears to be a feasible device for ob-

taining partial information on the heat flux transients in a flame. A simple, cheap, self-contained recorder, which measures current or voltage changes, is needed to make the device practical.

5. The gas-filled temperature probe does not appear to be suitable for measuring the temperature transients in a fire. It is slow to respond to changes in the environmental temperature and the need for a self-contained pressure recorder is an added disadvantage.

The following recommendations are made concerning future work:

1. Models of the most promising of the proposed devices, namely, the maximum temperature indicator, the fusible-rod integrated-heat flux meter, the fusible-rod differential-heat flux meter and the evaporative dosimeter should be constructed.
2. Laboratory tests should be performed on each of the model instruments for calibration and to evaluate the reliability of each of the devices.
3. Actual field testing should be performed on small numbers of the proposed devices.
4. Work should continue on finding similar and hopefully simpler devices for measuring or inferring the heat effects of a fire.

A SELECTED BIBLIOGRAPHY

1. Belcher, P. R., and R. W. Wilson. "Templugs," The Engineer, 221 (February 25, 1966), 305-308.

2. Boelter, L. M. K., H. A. Johnson., et. al. Heat Transfer Notes. Berkeley: University of California Press, 1948.

3. Countryman, C. M. "Mass Fire Characteristics in Large-Scale Tests," Fire Technology, 1 No. 4 (November, 1965), 303-317.

4. Eckert, E. R. G., and R. M. Drake, Jr. Heat and Mass Transfer. New York: McGraw-Hill, 1959.

5. Edwards, J. D., F. C. Frary, and Z. Jeffries. The Aluminum Industry. Vol. II: Aluminum Products and Their Fabrication. New York: McGraw-Hill, 1930.

6. Gallant, R. W. "Physical Properties of Hydrocarbons," Hydrocarbon Processing, 45 (March, 1966), 161-168.

7. Gallant, R. W. "Physical Properties of Hydrocarbons," Hydrocarbon Processing, 46 (April, 1967), 183-196.

8. Gallant, R. W. "Physical Properties of Hydrocarbons," Hydrocarbon Processing, 46 (May, 1967), 201-215.

9. Hadfield, D., ed. Permanent Magnets and Magnetism. New York: John Wiley & Sons, 1962.

10. Hougen, O. A., K. M. Watson, and R. A. Ragatz. Chemical Process Principles. 2nd ed. Vol. I: Material and Energy Balances. New York: John Wiley & Sons, 1962.

11. International Critical Tables. New York: McGraw-Hill, 1933.

12. Keenaw, J. H., and F. G. Keyes. Thermodynamic Properties of Steam. New York: John Wiley & Sons, 1936.

13. Kelley, K. K. U. S. Bureau of Mines Bulletin. 476, 1949.

14. Lange, N. A. ed. Handbook of Chemistry. 6th ed. Sandusky: Handbook Publishers, 1946.

15. McCarter, R. J., and A. Broido. "A Radiant Energy Dosimeter for Field Use," Fire Technology, 3 (August, 1967), 213-224.

16. Norden, R. B. "Formed Silica: Hard-to-Beat Properties," Chemical Engineering, 65 (August 25, 1958), 142-144.

17. Rosenthal, D. "The Theory of Moving Sources of Heat and Its Application to Metal Treatments," Trans. A.S.M.E., 68 (1946), 849-866.

18. Salvadori, M. G., and M. L. Baron. Numerical Methods in Engineering. 2nd ed. Englewood Cliffs: Prentice-Hall, 1961.

19. Southworth, R. W., and S. L. Deleeuw. Digital Computation and Numerical Methodes. New York: McGraw-Hill, 1965.

20. "Thermometry." Encyclopaedia Britannica. 1961. Vol. XXII.

21. Thomas, P. H. and P. G. Smith. "Simple Dosage Meter for High-Intensity Thermal Radiation," Journal of Scientific Instruments, 37 (March, 1960), 73-76.

22. Touloukian, Y. S., ed. Thermophysical Properties Research Literature Retrieval Guide. 2nd ed. New York: Plenum Press, 1967.

APPENDIX

NUMERICAL SOLUTION TO TRANSIENT HEAT CONDUCTION PROBLEM

In Chapter V the following conditions were imposed as criteria for calculating the insulation required to keep an instrument cool.

(a) The instrument and the surrounding insulation are initially at 80 F.

(b) The temperature at the inside surface of the insulation is not to exceed 200 F at any time.

(c) The surrounding temperature is 1000 F.

The insulation around the fusible-rod integrated-heat flux meter forms a hollow cylinder. Since the thermal conductivity of the insulation was low, the assumption was made that a good approximation to the required insulation thickness could be obtained with the aid of the Boelter charts for transient one-directional heat conduction in a solid cylinder. Thus, the time required to heat an imaginary surface at .3125 inches from the center of the solid insulation was calculated. The validity of calculating the insulation thickness or the heating time by this method will now be checked. The following numerical solution to the transient heat conduction problem is to be considered.

Figure 24 is a conceptual drawing of the insulation. The problem is to calculate the time required to heat the surface R_i to 200 F. Let the initial temperature throughout the hollow cylinder be some arbitrary function of the radius, $t_i(r)$. Imagine the temperature of the outer surface of insulation R_o to be suddenly raised to t_s and maintained at this value for all $\theta > 0$. An adiabatic surface is assumed to exist at R_i. This simplification will give a conservative answer for the insulation thickness; the calculated insulation thickness will be slightly greater than actually required.

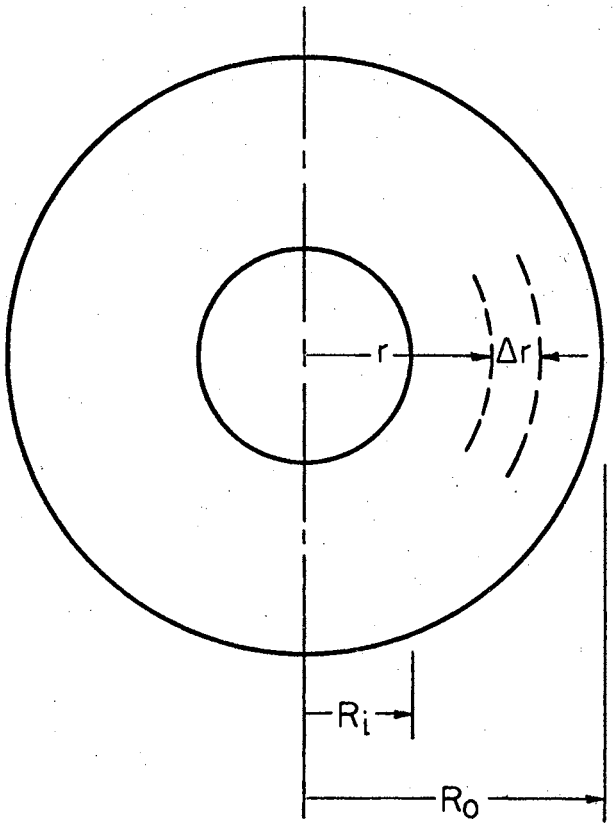

(a)

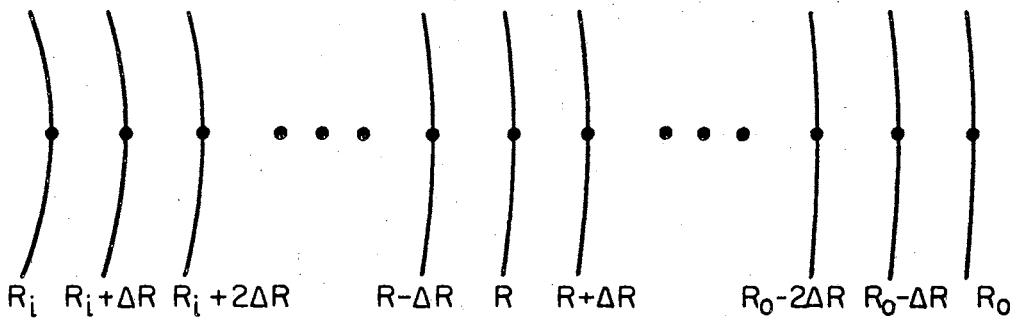

(b)

Figure 24. Cylindrical Insulation and Interval Representation

In this case the solution for $t(r,\theta)$ must satisfy

$$\frac{\partial^2 t}{\partial r^2} + \frac{1}{r}\frac{\partial t}{\partial r} = \frac{1}{\alpha}\frac{\partial t}{\partial \theta} \tag{1}$$

and the boundary conditions

(1) $t = t_o$ at $\theta = 0$; $R_i \leq r \leq R_o$

(2) $t = t_s$ at $\theta > 0$; $r = R_o$

(3) $\frac{\partial t}{\partial r} = 0$ at $r = R_i$; $\theta > 0$

Numerical approximations to the partial differential equation 1 and the third boundary condition are obtained by substituting finite-difference expressions for the derivatives. Central differences in space and forward differences in time are used in equation 1. Then

$$\frac{t_{\theta,R+\Delta R} + t_{\theta,R-\Delta R} - 2t_{\theta,R}}{(\Delta R)^2} + \frac{1}{R}\frac{t_{\theta,R+\Delta R} - t_{\theta,R-\Delta R}}{2(\Delta R)} = \frac{t_{\theta+\Delta\theta,R} - t_{\theta,R}}{\alpha(\Delta\theta)} \tag{2}$$

Forward differences in space are used to obtain the difference equation for the third boundary condition. Hence,

$$\frac{4t_{\theta,R_i+\Delta R} - t_{\theta,R_i+2\Delta R} - 3t_{\theta,R_i}}{2\Delta R} = 0 \tag{3}$$

Equations 2 and 3 are now rearranged to yield

$$t_{\theta+\Delta\theta,R} = t_{\theta,R} + \alpha(\Delta\theta)\left[\frac{t_{\theta,R+\Delta R} + t_{\theta,R-\Delta R} - 2t_{\theta,R}}{(\Delta R)^2} + \frac{1}{R}\frac{t_{\theta,R+\Delta R} - t_{\theta,R-\Delta R}}{2(\Delta R)}\right] \tag{4}$$

and

$$t_{\theta,R_i} = \frac{4t_{\theta,R_i+\Delta R} - t_{\theta,R_i+2\Delta R}}{3} \tag{5}$$

To solve equations 4 and 5 one initially assumes an insulation thickness. The insulation is then divided into equally spaced radii, as shown in Figure 24 (b), and a time increment $\Delta\theta$ is chosen. Starting at the node $R_{o-\Delta R}$ the future temperature $t_{\theta+\Delta\theta,R}$ is calculated for all nodes between and including the radii $R_{o-\Delta R}$ and $R_{i+\Delta R}$. Then the new temperature at the wall R_i is calculated by equation 5. Finally the temperatures at time θ are set equal to the temperatures at time $\theta+\Delta\theta$. The process is repeated for future times $\theta+n\Delta\theta$, where n = 1,2,3,... m. For further information on the solution of partial differential equations by numerical methods one is referred to the text by Salvadori and Baron (18).

Equations 4 and 5 were used to calculate the time required to heat the inner surface of various thicknesses of insulation. The heating times were calculated for insulation thicknesses of 1, 2, 3, 4 and 5 inches. For insulation thicknesses of 1, 2 and 3 inches, time increments of 6.0 seconds and radius increments of $(R_o-R_i)/10$ were chosen, while for the 4 and 5 inch thicknesses the time and radius increments were 12.0 seconds and $(R_o-R_i)/20$ respectively.

Equations 4 and 5 were programed for the IBM 7040 computer. The results of these calculations are compared with the Boelter solution in Figure 25. The numerical solution heating times are shown to be slightly less than the Boelter solution heating times. This was expected because no heat was allowed to pass into the center of the hollow cylinder from the boundary R_i in the numerical solution case. In practice some heat will be conducted past the boundary R_i and will increase the heating time slightly.

In conclusion, it appears that the Boelter charts for transient one-

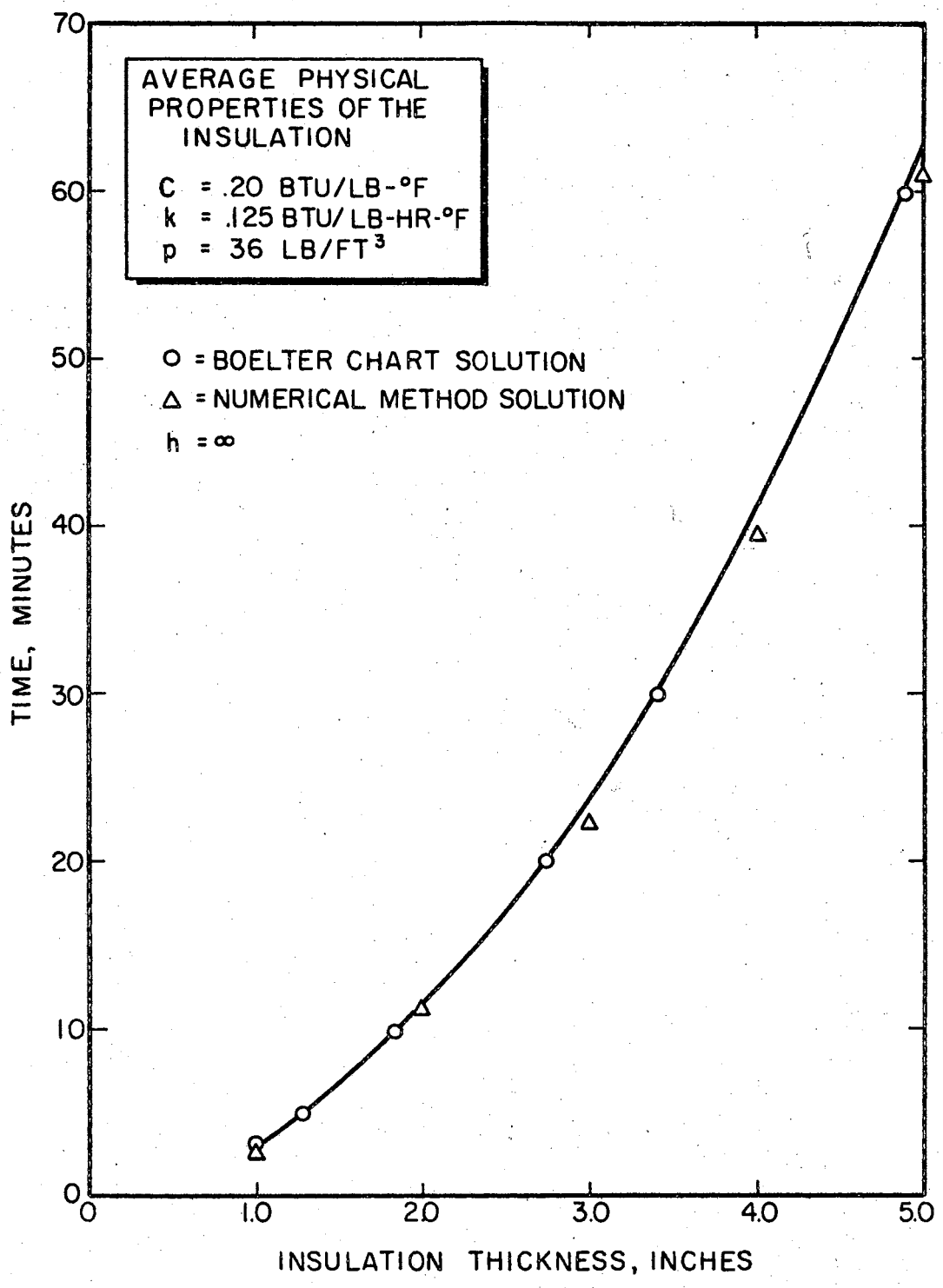

Figure 25. Comparison Between Boelter Chart Method and Finite-Difference Numerical Method for Calculating Insulation Thickness Around a 5/8" O.D. Tube

directional heat conduction in solid cylinders can be used to give a good approximation for the insulation thickness.

VITA

Duane Clark McCoy

Candidate for the Degree of

Master of Science

Thesis: SIMPLE INSTRUMENTATION FOR LARGE FIRES

Major Field: Chemical Engineering

Biographical:

Personal Data: Born in Effingham, Illinois, February 24, 1945, the son of Woodrow P. and Edna M. McCoy.

Education: Graduated from Thomas A. Edison High School, Tulsa, Oklahoma, in May, 1963; received the Bachelor of Science degree in Chemical Engineering from the University of Tulsa in 1967; attended Oklahoma State University in 1967 and 1968; completed requirements for the Master of Science degree at Oklahoma State University in May, 1969.

Professional Experience: Employed as an assistant engineer and computer programmer with Dale L. Gulley and Associates in Tulsa, Oklahoma during 1967 and 1968.